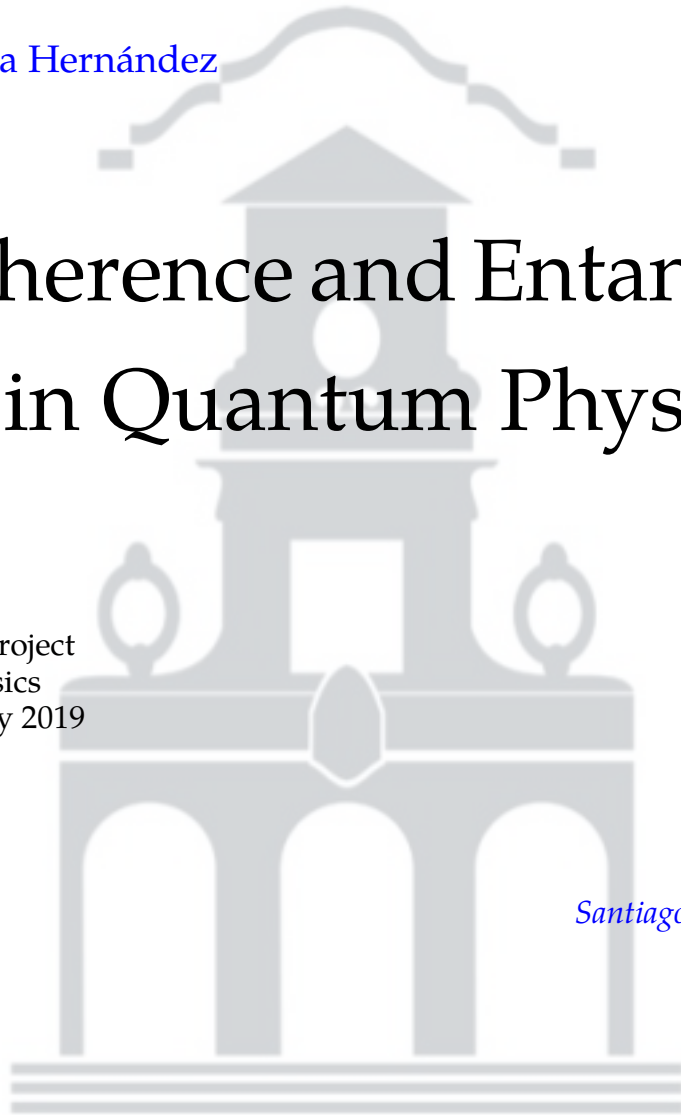


Jorge Medina Hernández

Decoherence and Entanglement in Quantum Physics

Final Degree Project
Degree in Physics
La Laguna, July 2019

DIRECTED BY
Santiago Brouard Martín



Santiago Brouard Martín
Department of Applied Physics
University of La Laguna
38206 La Laguna, Tenerife

Acknowledgements

A Santiago, por su ayuda y dedicación a lo largo de este trabajo.

A todos los profesores, por lo aprendido en estos cuatro años.

A mi familia y también a mis amigos, por el apoyo incondicional que siempre han mostrado.

Abstract · Resumen

Abstract

Throughout this project, the case of a composite system formed by a harmonic oscillator and a two-state atom will be studied; considering both affect each other as a consequence of a Jaynes-Cummings interaction, and being both coupled to different reservoirs that are assumed to be independent from each other. The effects of the decoherence in the evolution of the populations and coherences will be analyzed; specifically the energy dissipation and the coherence loss, as well as the stationary states and the relevance of the Jaynes-Cummings interaction. Finally, the solution of stochastic equations will be analyzed, particularly the evolution of the expectation value of the position operator for the harmonic oscillator; for the case of simultaneous measurements in both subsystems, as well as for a measurement in the harmonic oscillator when the two-state atom undergoes a decoherence process.

Keywords: *Decoherence – entanglement – master equation – stochastic master equation – continuous quantum measurement.*

Resumen

En este trabajo se estudiará un sistema compuesto por un oscilador armónico y un átomo de dos niveles que presentan una interacción del tipo Jaynes-Cummings, estando cada uno acoplado a un reservorio y asumiendo que éstos son independientes entre sí. Se analizarán los efectos de la decoherencia en la evolución de poblaciones y coherencias; específicamente la disipación de energía y la pérdida de coherencia, así como los estados estacionarios y la relevancia de la interacción de Jaynes Cummings. Finalmente, se examinará la solución de ecuaciones estocásticas, concretamente la evolución del valor esperado de la posición para el oscilador armónico, cuando se realiza una medida simultánea en el sistema de dos niveles; y cuando únicamente se mide éste y el átomo de dos niveles experimenta decoherencia.

Palabras clave: *Decoherencia – entrelazamiento – ecuación maestra – ecuación maestra estocástica – medida cuántica continua.*

Contents

Acknowledgements	iii
Abstract · Resumen	v
1 Introduction	1
2 Objectives	3
3 Master equation	4
3.1 Derivation	4
3.2 Born approximation	5
3.3 Markoff approximation	6
4 Interacting systems coupled to reservoirs.	7
4.1 Master equation	8
4.2 Stationary states	13
4.3 Numerical solution	15
4.3.1 Pure state at $T=0K$	16
4.3.2 Entangled state at $T \neq 0K$	19
5 Stochastic equation	22
5.1 Derivation	23
5.2 Measurement on interacting systems via reservoirs	27
5.2.1 SME derivation	28
5.2.2 Numerical solution	32
5.3 Measurement and decoherence	33
5.3.1 Numerical solution	34
6 Conclusions	35
List of Figures	37
List of Tables	37
References	38

1 Introduction

La mecánica cuántica es una de las teorías más exitosas de la física, generalmente utilizada en el ámbito microscópico. Una de sus líneas de investigación estudia la transición desde la mecánica cuántica a la clásica, pudiendo considerarse esta última como un caso particular de la primera. De este modo, la decoherencia emerge como un proceso que explica esta transición, concretamente a través de la interacción de un sistema \mathcal{S} con su entorno \mathcal{R} , siendo por tanto \mathcal{S} un sistema abierto. Específicamente, el mecanismo provocaría una pérdida de coherencia en el sistema, ligada a la aparición de una base privilegiada para la matriz densidad, que puede explicar la aparición de únicamente resultados clásicos cuando se lleva a cabo una medida.

Quantum mechanics is one of the most successful theories in Physics, since no experiment has ever contradicted its predictions. It is generally accepted its proficiency at the microscopic level, while classical physics is often associated with the macroscopic regime. However, this is not a valid criteria, since in some cases such as the cryogenic version of the Weber bar –a gravity-wave detector–, the device must be treated as a quantum harmonic oscillator despite weighting about a ton. Therefore, the previous explanation is proven to be not accurate enough. A crucial difference between the two arises from the quantum superposition principle, which allows a system to be in a coherent superposition of states that account for different potential outcomes, rather than in a classical, defined state.

In quantum mechanics, the time evolution of a system \mathcal{S} is given by Schrödinger's equation, which is only applicable to closed systems and produces an unitary evolution, causing \mathcal{S} to remain as a pure state. Nevertheless, macroscopic systems are always interacting with their environment \mathcal{R} and, consequently, \mathcal{S} will experience a loss of coherence (decoherence) that leaks into \mathcal{R} . Hence, the system will no longer stay in a superposition of states and only the classical outcome would be perceived. This process, which accounts for the non-unitary evolution caused by the leak of information, is the so called *decoherence*, one of the most renowned approaches to describe the transition from quantum to classical mechanics.

In order to explain this process, let us consider a two-state system \mathcal{S} and a two-state detector \mathcal{D} , with orthonormal basis $\{|\uparrow\rangle, |\downarrow\rangle\}$ and $\{|d_\uparrow\rangle, |d_\downarrow\rangle\}$, respectively, as described in [1]. The detector remains in the $|d_\downarrow\rangle$ state until \mathcal{S} has spin state $|\uparrow\rangle$:

$$|\downarrow\rangle|d_\downarrow\rangle \rightarrow |\downarrow\rangle|d_\downarrow\rangle, \quad |\uparrow\rangle|d_\downarrow\rangle \rightarrow |\uparrow\rangle|d_\uparrow\rangle. \quad (1.1)$$

Before the interaction, we can consider \mathcal{S} to be in a general pure state $|\psi_S\rangle$ such that the initial state of the total system $|\Phi^i\rangle$ is given by

$$|\Phi^i\rangle = |\psi_S\rangle|d_\downarrow\rangle = (\alpha|\uparrow\rangle + \beta|\downarrow\rangle)|d_\downarrow\rangle. \quad (1.2)$$

Due to the interaction (1.1), the initial state evolves into a correlated state $|\Phi^c\rangle$:

$$|\Phi^i\rangle = \alpha|\uparrow\rangle|d_\downarrow\rangle + \beta|\downarrow\rangle|d_\downarrow\rangle \rightarrow |\Phi^c\rangle = \alpha|\uparrow\rangle|d_\uparrow\rangle + \beta|\downarrow\rangle|d_\downarrow\rangle \equiv \alpha|\uparrow, d_\uparrow\rangle + \beta|\downarrow, d_\downarrow\rangle. \quad (1.3)$$

Therefore, it seems that if the detector is seen to be in the state $|d_\uparrow\rangle$ or $|d_\downarrow\rangle$, we can conclude that \mathcal{S} will be in $|\uparrow\rangle$ or $|\downarrow\rangle$, respectively. However, since the state of both systems can not be described as the product of a state $|\phi_{S_1}\rangle \in \mathcal{H}_{S_1}$ and $|\phi_{S_2}\rangle \in \mathcal{H}_{S_2}$; even if the total system is in a pure state, the subsystems will be in mixed states and hence we should examine the density matrix of the system:

$$\rho^c = |\Phi^c\rangle\langle\Phi^c| = |\alpha|^2|\uparrow, d_\uparrow\rangle\langle\uparrow, d_\uparrow| + \alpha\beta^*|\uparrow, d_\uparrow\rangle\langle\downarrow, d_\downarrow| + \alpha^*\beta|\downarrow, d_\downarrow\rangle\langle\uparrow, d_\uparrow| + |\beta|^2|\downarrow, d_\downarrow\rangle\langle\downarrow, d_\downarrow|. \quad (1.4)$$

The presence of non-diagonal terms, the exclusively quantum correlations (entanglement), indicates that the outcomes are not independent of each other. If we neglect them, we would obtain the reduced density matrix,

$$\rho^r = |\alpha|^2|\uparrow, d_\uparrow\rangle\langle\uparrow, d_\uparrow| + |\beta|^2|\downarrow, d_\downarrow\rangle\langle\downarrow, d_\downarrow|, \quad (1.5)$$

where now the coefficients can be interpreted as classical probabilities and we can, even when not knowing the result of a measurement, safely predict which are the possible outcomes. We may show that this is not the case for ρ^c by taking $\alpha = -\beta = 1/\sqrt{2}$:

$$|\Phi^c\rangle = \frac{1}{\sqrt{2}}(|\uparrow, d_\uparrow\rangle - |\downarrow, d_\downarrow\rangle). \quad (1.6)$$

Since this state is invariant under basis rotations, we can rewrite it in terms of the eigenstates of $\hat{\sigma}_x$:

$$|\odot\rangle = \frac{1}{\sqrt{2}}(|\uparrow\rangle + |\downarrow\rangle), \quad |\otimes\rangle = \frac{1}{\sqrt{2}}(|\uparrow\rangle - |\downarrow\rangle). \quad (1.7)$$

Performing similar transformations for the states of the detector, we get

$$|\Phi^c\rangle = -\frac{1}{\sqrt{2}}(|\odot, d_\odot\rangle - |\otimes, d_\otimes\rangle). \quad (1.8)$$

We find that the states appearing on the diagonal of ρ^c according to the previous equation and the one we would obtain by choosing $\alpha = -\beta = 1/\sqrt{2}$ in (1.4) do not coincide:

$$\rho_{\text{diag}}^c = \frac{1}{2}(|\uparrow, d_\uparrow\rangle\langle\uparrow, d_\uparrow| + |\downarrow, d_\downarrow\rangle\langle\downarrow, d_\downarrow|) = \frac{1}{2}(|\odot, d_\odot\rangle\langle\odot, d_\odot| + |\otimes, d_\otimes\rangle\langle\otimes, d_\otimes|). \quad (1.9)$$

As we said before, the state (1.6) is invariant under basis rotations, and therefore we could get infinitely many different expressions for ρ_{diag}^c , which indicates that the set of alternative outcomes is not determined by ρ^c . However, if we consider the composite system \mathcal{SD} to be embedded in an environment \mathcal{E} that correlates with the state of the detector analogously to the $\mathcal{S} - \mathcal{D}$ interaction (1.1):

$$|\Psi^i\rangle = |\Phi^c\rangle|\mathcal{E}_0\rangle = (\alpha|\uparrow, d_\uparrow\rangle + \beta|\downarrow, d_\downarrow\rangle)|\mathcal{E}_0\rangle \rightarrow |\Psi^c\rangle = \alpha|\uparrow, d_\uparrow, \mathcal{E}_\uparrow\rangle + \beta|\downarrow, d_\downarrow, \mathcal{E}_\downarrow\rangle, \quad (1.10)$$

then, assuming the environment states associated to the detector states $\{|d_\uparrow\rangle, |d_\downarrow\rangle\}$ to be orthonormal: $\langle \mathcal{E}_i | \mathcal{E}_j \rangle = \delta_{ij}$, we can obtain the density matrix for \mathcal{SD} by tracing over the environment degrees of freedom:

$$\rho_{\mathcal{DS}} = \text{Tr}_{\mathcal{E}} |\Psi^c\rangle\langle\Psi^c| = \sum_i \langle \mathcal{E}_i | \Psi^c \rangle \langle \Psi^c | \mathcal{E}_i \rangle = |\alpha|^2 |\uparrow, d_\uparrow\rangle\langle\uparrow, d_\uparrow| + |\beta|^2 |\downarrow, d_\downarrow\rangle\langle\downarrow, d_\downarrow| = \rho^r. \quad (1.11)$$

We have obtained the reduced density matrix without performing any non-unitary processes, and moreover, a preferred basis of the detector has appeared, often called the *pointer basis*. In other words, the decoherence mechanism by which the system \mathcal{SD} experiences a loss of coherence through the interaction with an environment \mathcal{E} , provides an explanation for the appearance of only the classical outcomes when performing a measurement.

2 Objectives

El trabajo constará de dos partes. En primera instancia se estudiará un sistema compuesto por un oscilador armónico y un átomo de dos niveles que interactúan entre sí. Además, estarán acoplados a sendos sistemas de un número elevado de grados de libertad, denominados reservorios, que consideraremos independientes; y que darán lugar a un proceso de decoherencia descrito por ecuaciones maestras. Posteriormente se procederá a analizar ecuaciones estocásticas, que describen la evolución temporal de sistemas causada por la medida de un observable. En concreto, se analizará el valor esperado del operador de posición del oscilador armónico para dos casos: la medida simultánea en el átomo de dos niveles, y su medida única cuando el sistema de dos niveles está sujeto a decoherencia.

The project will be divided in two sections. First, a system formed by a harmonic oscillator and a two-state system which interact between them will be analyzed. We will consider each subsystem to be coupled to a system with a high number of degrees of freedom (reservoir), and both reservoirs will be assumed to be independent. This coupling will lead to a decoherence process, described by master equations. Afterwards, we will proceed to evaluate stochastic equations, which describe the time evolution of systems caused by the measurement of an observable. Specifically, the evolution of the expectation value of the position operator for the harmonic oscillator will be examined for two cases: a simultaneous measurement in the two-state system, and solely its measurement when the two-state atom is under a decoherence process.

3 Master equation

Una ecuación maestra es un conjunto de ecuaciones diferenciales de primer orden, que describe la evolución de los elementos de la matriz densidad para un sistema abierto acoplado a un reservorio. En primer lugar llevaremos a cabo su derivación general, para luego aplicarla a un caso particular.

A master equation is a set of first-order differential equations, which describes the time evolution of the elements of the density matrix for an open quantum system coupled to a reservoir. We will follow [2] for its derivation and will later proceed to study its form and solution for a specific case.

3.1 Derivation

The ensemble composed by a system \mathcal{S} and a reservoir \mathcal{R} is generally described by a Hamiltonian¹ of the form

$$H = H_S + H_R + H_{SR}, \quad (3.1)$$

where H_S and H_R are the Hamiltonians for \mathcal{S} and \mathcal{R} , respectively; and H_{SR} is the interaction Hamiltonian. The time evolution of the density operator for the global system, $\chi(t)$, is given by

$$i\hbar \frac{d}{dt} \chi(t) = [H, \chi]. \quad (3.2)$$

Performing a transformation into the interaction picture:

$$\tilde{\chi}(t) = e^{\frac{i}{\hbar}(H_S+H_R)t} \chi(t) e^{-\frac{i}{\hbar}(H_S+H_R)t}, \quad (3.3)$$

equation (3.2) results in

$$\dot{\tilde{\chi}}(t) = \frac{1}{i\hbar} [\tilde{H}_{SR}(t), \tilde{\chi}(t)], \quad (3.4)$$

which can be integrated to give

$$\tilde{\chi}(t) = \chi(0) + \frac{1}{i\hbar} \int_0^t dt' [\tilde{H}_{SR}(t'), \tilde{\chi}(t')]. \quad (3.5)$$

Substituting the previous equation in (3.4) we get

$$\dot{\tilde{\chi}} = \frac{1}{i\hbar} [\tilde{H}_{SR}(t), \chi(0)] - \frac{1}{\hbar^2} \int_0^t dt' [\tilde{H}_{SR}(t), [\tilde{H}_{SR}(t'), \tilde{\chi}(t')]]. \quad (3.6)$$

Since we are interested in the features of the system \mathcal{S} , we will study the evolution of the reduced density operator $\rho(t)$, obtained by taking the partial trace over the reservoir states:

¹To simplify the notation we will use $O \equiv \hat{O}$, where \hat{O} is a general operator.

$$\dot{\tilde{\rho}} = \text{Tr}_R(\dot{\tilde{\chi}}) = \text{Tr}_R\left(\frac{1}{i\hbar}[\tilde{H}_{SR}(t), \chi(0)]\right) - \text{Tr}_R\left(\frac{1}{\hbar^2} \int_0^t dt' [\tilde{H}_{SR}(t), [\tilde{H}_{SR}(t'), \tilde{\chi}(t')]]\right). \quad (3.7)$$

If we consider that the interaction is turned on at $t = 0$, then no correlations exists between \mathcal{S} and \mathcal{R} at the initial time and the density operator can be factorized as

$$\chi(0) = \rho_0 R_0, \quad (3.8)$$

where ρ_0 and R_0 are the initial density operators for the system and the reservoir, respectively. We find that the first term in (3.7) can be eliminated under the assumption of reservoir operators coupling to \mathcal{S} (Γ_i) having zero mean value in the initial reservoir state, since

$$\begin{aligned} \text{Tr}_R[\tilde{H}_{SR}(t)\rho_0 R_0] &= \text{Tr}_R\left[\hbar \sum_i e^{\frac{i}{\hbar}H_S t} s_i e^{-\frac{i}{\hbar}H_S t} e^{\frac{i}{\hbar}H_R t} \Gamma_i e^{-\frac{i}{\hbar}H_R t} \rho_0 R_0\right] \\ &= \hbar \rho_0 \sum_i s_i(t) \text{Tr}_R[\Gamma_i(t)R_0] = \hbar \rho_0 \sum_i s_i(t) \langle \Gamma_i(t) \rangle_{R_0}. \end{aligned} \quad (3.9)$$

If $\langle \Gamma_i(t) \rangle_{R_0} \neq 0$, the equality can be arranged by redefining the system's and the interaction Hamiltonians as

$$H'_S = H_S + \text{Tr}_R(H_{SR}R_0), \quad H'_{SR} = H_{SR} - \text{Tr}_R(H_{SR}R_0). \quad (3.10)$$

Thus,

$$\dot{\tilde{\rho}} = -\frac{1}{\hbar^2} \int_0^t dt' \text{Tr}_R[\tilde{H}_{SR}(t), [\tilde{H}_{SR}(t'), \tilde{\chi}(t')]]. \quad (3.11)$$

This equation is still exact and contains the same information about the system evolution as (3.2), since no approximations have been made so far.

3.2 Born approximation

We have stated the factorization of $\tilde{\chi}$ at $t=0$. However, when time increases correlations between \mathcal{S} and \mathcal{R} may appear due to the coupling of both systems through H_{SR} . If we consider the reservoir to be much larger than \mathcal{S} , its state should barely be affected by the coupling and hence \mathcal{R} is assumed to be in a stationary state, which verifies

$$\tilde{R}(t) \approx \tilde{R}(0) = R_0, \quad [R_0, H_R] = 0. \quad (3.12)$$

Furthermore, in a weak coupling scheme, at all times $\tilde{\chi}(t)$ may only lead to deviations of order H_{SR} from an uncorrelated state:

$$\tilde{\chi}(t) \simeq \tilde{\rho}(t)R_0 + \mathcal{O}(H_{SR}). \quad (3.13)$$

In the Born approximation, higher than second order terms in H_{SR} are neglected when substituting the previous equation in (3.11), which gives

$$\dot{\tilde{\rho}} \approx -\frac{1}{\hbar^2} \int_0^t dt' \text{Tr}_R \left[\tilde{H}_{SR}(t), [\tilde{H}_{SR}(t'), \tilde{\rho}(t') R_0] \right]. \quad (3.14)$$

3.3 Markoff approximation

A system is defined to be Markoffian when its future behaviour is determined only by its present state. Hence, equation (3.14) is non-Markoffian because the evolution of $\tilde{\rho}(t)$ depends on its past values due to the integration over $\tilde{\rho}(t')$. The Markoff approximation consists precisely in the replacement $\tilde{\rho}(t') \rightarrow \tilde{\rho}(t)$, which leads to the master equation in the Born-Markoff approximation:

$$\dot{\tilde{\rho}} \approx -\frac{1}{\hbar^2} \int_0^t dt' \text{Tr}_R \left[\tilde{H}_{SR}(t), [\tilde{H}_{SR}(t'), \tilde{\rho}(t) R_0] \right]. \quad (3.15)$$

In rigorous terms, \mathcal{S} will depend on its past history, since its previous states would affect the reservoir state due to the coupling H_{SR} ; which in turn will influence the evolution of \mathcal{S} through the interaction with the modified reservoir. Nevertheless, in the case we are considering, where \mathcal{R} is significantly larger than \mathcal{S} , the small changes in the reservoir are not expected to last for long enough to alter the future evolution of \mathcal{S} .

We can obtain the master equation in terms of operators by considering a general interaction Hamiltonian

$$H_{SR} = \hbar \sum_i s_i \Gamma_i, \quad (3.16)$$

where $s_i \in \mathcal{H}_S$ and $\Gamma_i \in \mathcal{H}_R$. Therefore

$$\tilde{H}_{SR}(t) = \hbar \sum_i \tilde{s}_i(t) \tilde{\Gamma}_i(t), \quad (3.17)$$

which substituted in the master equation in the Born approximation (3.14) gives

$$\begin{aligned} \dot{\tilde{\rho}} &= -\sum_{i,j} \int_0^t dt' \text{Tr}_R \left\{ \left[\tilde{s}_i(t) \tilde{\Gamma}_i(t), [\tilde{s}_j(t') \tilde{\Gamma}_j(t'), \tilde{\rho}(t') R_0] \right] \right\} \\ &= -\sum_{i,j} \int_0^t dt' \left\{ \left[\tilde{s}_i(t) \tilde{s}_j(t') \tilde{\rho}(t') - \tilde{s}_j(t') \tilde{\rho}(t') \tilde{s}_i(t) \right] \langle \tilde{\Gamma}_i(t) \tilde{\Gamma}_j(t') \rangle_R \right. \\ &\quad \left. + \left[\tilde{\rho}(t') \tilde{s}_j(t') \tilde{s}_i(t) - \tilde{s}_i(t) \tilde{\rho}(t') \tilde{s}_j(t') \right] \langle \tilde{\Gamma}_j(t') \tilde{\Gamma}_i(t) \rangle_R \right\}, \end{aligned} \quad (3.18)$$

being

$$\langle \tilde{\Gamma}_i(t) \tilde{\Gamma}_j(t') \rangle_R = \text{Tr}_R [R_0 \tilde{\Gamma}_i(t) \tilde{\Gamma}_j(t')], \quad \langle \tilde{\Gamma}_j(t') \tilde{\Gamma}_i(t) \rangle_R = \text{Tr}_R [R_0 \tilde{\Gamma}_j(t') \tilde{\Gamma}_i(t)]. \quad (3.19)$$

Thereby, the effects of the reservoir appear through (3.19). In relation with the Markoff approximation, we can uphold the replacement $\tilde{\rho}(t') \rightarrow \tilde{\rho}(t)$ if these correlations promptly decay compared to the characteristic time in which $\tilde{\rho}(t)$ varies. In the ideal case

$$\langle \tilde{\Gamma}_i(t) \tilde{\Gamma}_j(t') \rangle_R \propto \delta(t - t'). \quad (3.20)$$

Equation (3.18) dictates the general shape of a master equation. In order to obtain its explicit form, it is necessary to specify the total system under study, $\mathcal{S} \oplus \mathcal{R}$, as well as the corresponding Hamiltonian.

4 Interacting systems coupled to reservoirs.

Analizaremos en este punto la aplicación de las ecuaciones maestras al caso particular de un sistema compuesto por un oscilador armónico y un átomo de dos niveles, que presentan una interacción del tipo Jaynes-Cummings. Los subsistemas se encontrarán acoplados cada uno a un reservorio, siendo estos independientes. Concretamente, se estudiará la evolución de las poblaciones y coherencias para distintos estados iniciales y temperaturas, así como la aparición de estados estacionarios.

We will study the case of a system $\mathcal{S} = \mathcal{S}_1 \oplus \mathcal{S}_2$, where \mathcal{S}_1 and \mathcal{S}_2 correspond to a harmonic oscillator and a two-state atom, respectively; which affect each other through a Jaynes-Cumming's interaction H_{JC} . Furthermore, the subsystem \mathcal{S}_1 is coupled to a reservoir \mathcal{R}_1 , which is a collection of harmonic oscillators; and \mathcal{S}_2 couples to the electromagnetic field \mathcal{R}_2 . Considering both reservoirs to be independent, the total Hamiltonian is given by

$$H = H_S + H_R + H_{SR} = H_{S_1} + H_{S_2} + H_{JC} + H_{R_1} + H_{R_2} + H_{S_1 R_1} + H_{S_2 R_2}, \quad (4.1)$$

being

$$\begin{aligned} H_{S_1} &= \hbar\omega_c a^\dagger a, & H_{S_2} &= \frac{1}{2} \hbar\omega_A \sigma_z, \\ H_{R_1} &= \sum_j \hbar\omega_j r_j^\dagger r_j, & H_{R_2} &= \sum_{\mathbf{k}\lambda} \hbar\omega_{\mathbf{k}} r_{\mathbf{k}\lambda}^\dagger r_{\mathbf{k}\lambda}, \\ H_{S_1 R_1} &= \sum_j \hbar(\kappa_j^* a r_j^\dagger + \kappa_j a^\dagger r_j) \equiv \hbar(a\Gamma_1^\dagger + a\Gamma_1), \\ H_{S_2 R} &= \sum_{\mathbf{k}\lambda} \hbar(\kappa_{\mathbf{k}\lambda}^{*(2)} \sigma_- r_{\mathbf{k}\lambda}^\dagger + \kappa_{\mathbf{k}\lambda}^{(2)} \sigma_+ r_{\mathbf{k}\lambda}) \equiv \hbar(\sigma_- \Gamma_2^\dagger + \sigma_+ \Gamma_2), \\ H_{JC} &= \hbar(da^\dagger \sigma_- + d^* a \sigma_+), \end{aligned} \quad (4.2)$$

where a and a^\dagger are the annihilation and creation operators for the harmonic oscillator with frequency ω_c ; r_j and r_j^\dagger are those for the harmonic oscillators of the reservoir \mathcal{R}_1

with frequencies ω_j ; $r_{\mathbf{k}\lambda}$ and $r_{\mathbf{k}\lambda}^\dagger$ are the equivalent for \mathcal{R}_2 , a collection of oscillators (electromagnetic field modes) with frequencies $\omega_{\mathbf{k}}$, wave vectors \mathbf{k} and polarization states λ ; and σ_z , σ_+ and σ_- are *pseudo*-spin operators for the two-state system with energy difference $\hbar\omega_A$. Furthermore, the strength of the coupling between \mathcal{S}_1 and the j^{th} oscillator of \mathcal{R}_1 is characterized by the coupling constant κ_j ; $\kappa_{\mathbf{k}\lambda}$ is the coupling constant for the coupling between \mathcal{S}_2 and a photon characterized by \mathbf{k} and λ ; and d corresponds to the coupling constant for the interaction between \mathcal{S}_1 and \mathcal{S}_2 .

We have used the dipole approximation ($e^{i\mathbf{k}\cdot\mathbf{r}} \approx 1$) for the interaction between \mathcal{S}_2 and \mathcal{R}_2 ; as well as the rotating wave approximation for every interaction Hamiltonian, where we neglect the counter-rotating terms that do not conserve energy (i.e. $a^\dagger\sigma_+$) and average out to zero in the time scale in which \mathcal{S} varies. In the interaction picture for the \mathcal{S}_1 - \mathcal{S}_2 interaction, this implies neglecting fastly oscillating terms, proportional to $e^{\pm i(\omega_A + \omega_c)t}$, and preserve those of the form $e^{\pm i(\omega_a - \omega_c)t}$; an approximation which is better the more similar the frequencies from both systems are. For this reason, from now on we will consider

$$\omega_c = \omega_A \equiv \omega_S. \quad (4.3)$$

Since we are considering both reservoirs to be in thermal equilibrium at temperature T , their density operators will be given by

$$R_0^{(1)} = \prod_j e^{-\hbar\omega_j r_j^\dagger r_j / k_B T} \left(1 - e^{-\hbar\omega_j / k_B T}\right), \quad R_0^{(2)} = \prod_{\mathbf{k}\lambda} e^{-\hbar\omega_{\mathbf{k}} r_{\mathbf{k}\lambda}^\dagger r_{\mathbf{k}\lambda} / k_B T} \left(1 - e^{-\hbar\omega_{\mathbf{k}} / k_B T}\right). \quad (4.4)$$

4.1 Master equation

We will now explicitly obtain the master equation in the Born-Markoff approximation (3.18) for this particular case. We can make the identifications

$$s_j \in \{a, a^\dagger, \sigma_-, \sigma_+\}, \quad \Gamma_j \in \{\Gamma_1, \Gamma_1^\dagger, \Gamma_2, \Gamma_2^\dagger\}. \quad (4.5)$$

In the interaction picture corresponding to the H_{SR} interaction, the operators are given by

$$\begin{aligned} \tilde{s}_j(t) &= e^{\frac{i}{\hbar}(\sum_k H_{R_k} + \sum_n H_{S_n})} s_j e^{-\frac{i}{\hbar}(\sum_k H_{R_k} + \sum_n H_{S_n})} = e^{\frac{i}{\hbar}H_{S_j}} s_j e^{-\frac{i}{\hbar}H_{S_j}}, \\ \tilde{\Gamma}_j(t) &= e^{\frac{i}{\hbar}(\sum_k H_{R_k} + \sum_n H_{S_n})} \Gamma_j e^{-\frac{i}{\hbar}(\sum_k H_{R_k} + \sum_n H_{S_n})} = e^{\frac{i}{\hbar}H_{R_j}} \Gamma_j e^{-\frac{i}{\hbar}H_{R_j}}, \end{aligned} \quad (4.6)$$

since operators that act in different Hilbert spaces commute. Hence:

$$\begin{aligned} \tilde{a}(t) &= a e^{-i\omega_S t}, & \tilde{a}^\dagger(t) &= a^\dagger e^{i\omega_S t}, \\ \tilde{\sigma}_-(t) &= \sigma_- e^{-i\omega_S t}, & \tilde{\sigma}_+(t) &= \sigma_+ e^{i\omega_S t}, \\ \tilde{\Gamma}_1(t) &= \sum_j \kappa_j r_j e^{-i\omega_j t}, & \tilde{\Gamma}_1^\dagger(t) &= \sum_j \kappa_j^* r_j^\dagger e^{i\omega_j t}, \\ \tilde{\Gamma}_2(t) &= \sum_{\mathbf{k}\lambda} \kappa_{\mathbf{k}\lambda} r_{\mathbf{k}\lambda} e^{-i\omega_{\mathbf{k}} t}, & \tilde{\Gamma}_2^\dagger(t) &= \sum_{\mathbf{k}\lambda} \kappa_{\mathbf{k}\lambda}^* r_{\mathbf{k}\lambda}^\dagger e^{i\omega_{\mathbf{k}} t}, \end{aligned} \quad (4.7)$$

where we have applied the Baker–Campbell–Hausdorff formula:

$$e^A B e^{-A} = B + [A, B] + \frac{1}{2!} [A, [A, B]] + \dots \quad (4.8)$$

As an example, the calculation for $\tilde{a}(t)$ will be shown:

$$\begin{aligned} \tilde{a}(t) &= e^{i\omega_S a^\dagger a t} a e^{-i\omega_S a^\dagger a t} = a + i\omega_S t [a^\dagger a, a] + \frac{(i\omega_S t)^2}{2!} [a^\dagger a, [a^\dagger a, a]] + \dots \\ &= a \left(1 - i\omega_S t + \frac{(-i\omega_S t)^2}{2!} + \dots \right) = a e^{-i\omega_S t}, \end{aligned} \quad (4.9)$$

obtained using the commutation relation $[a^\dagger a, a] = -a$. Now, since $i, j = 1, 2, 3, 4$ back in (3.18), there will be 256 terms in the summation. Nevertheless, most of them will not contribute to the integral due to the reservoir correlation functions:

$$\begin{aligned} \langle \tilde{\Gamma}_1^\dagger(t) \tilde{\Gamma}_1^\dagger(t') \rangle_R &= \sum_j (\kappa_j^*)^2 e^{i\omega_j(t+t')} \langle r_j^\dagger r_j^\dagger \rangle_{R_1} = \sum_j (\kappa_j^*)^2 e^{i\omega_j(t+t')} \langle r_j^\dagger r_j^\dagger \rangle_{R_1} = 0, \\ \langle \tilde{\Gamma}_1(t) \tilde{\Gamma}_1(t') \rangle_R &= \sum_j (\kappa_j)^2 e^{i\omega_j(t+t')} \langle r_j r_j \rangle_{R_1} = 0, \\ \langle \tilde{\Gamma}_1^\dagger(t) \tilde{\Gamma}_1(t') \rangle_R &= \sum_1 |\kappa_j|^2 e^{i\omega_j(t-t')} \langle r_j^\dagger r_j \rangle_{R_1} = \sum_j |\kappa_j|^2 e^{i\omega_j(t-t')} \bar{n}_1(\omega_j, T), \\ \langle \tilde{\Gamma}_1(t) \tilde{\Gamma}_1^\dagger(t') \rangle_R &= \sum_j |\kappa_j|^2 e^{-i\omega_j(t-t')} \langle r_j r_j^\dagger \rangle_{R_1} = \sum_j |\kappa_j|^2 e^{i\omega_j(t-t')} [\bar{n}_1(\omega_j, T) + 1] \end{aligned} \quad (4.10)$$

and

$$\begin{aligned} \langle \tilde{\Gamma}_2^\dagger(t) \tilde{\Gamma}_2^\dagger(t') \rangle_R &= \sum_{\mathbf{k}\lambda} (\kappa_{\mathbf{k}\lambda}^*)^2 e^{i\omega_{\mathbf{k}}(t+t')} \langle r_{\mathbf{k}\lambda}^\dagger r_{\mathbf{k}\lambda}^\dagger \rangle_{R_2} = 0, \\ \langle \tilde{\Gamma}_2(t) \tilde{\Gamma}_2(t') \rangle_R &= \sum_{\mathbf{k}\lambda} (\kappa_{\mathbf{k}\lambda})^2 e^{-i\omega_{\mathbf{k}}(t+t')} \langle r_{\mathbf{k}\lambda} r_{\mathbf{k}\lambda} \rangle_{R_2} = 0, \\ \langle \tilde{\Gamma}_2^\dagger(t) \tilde{\Gamma}_2(t') \rangle_R &= \sum_{\mathbf{k}\lambda} |\kappa_{\mathbf{k}\lambda}|^2 e^{i\omega_{\mathbf{k}}(t-t')} \langle r_{\mathbf{k}\lambda}^\dagger r_{\mathbf{k}\lambda} \rangle_{R_2} = \sum_{\mathbf{k}\lambda} |\kappa_{\mathbf{k}\lambda}|^2 e^{i\omega_{\mathbf{k}}(t-t')} \bar{n}_2(\omega_{\mathbf{k}}, T), \\ \langle \tilde{\Gamma}_2(t) \tilde{\Gamma}_2^\dagger(t') \rangle_R &= \sum_{\mathbf{k}\lambda} |\kappa_{\mathbf{k}\lambda}|^2 e^{-i\omega_{\mathbf{k}}(t-t')} \langle r_{\mathbf{k}\lambda} r_{\mathbf{k}\lambda}^\dagger \rangle_{R_2} = \sum_{\mathbf{k}\lambda} |\kappa_{\mathbf{k}\lambda}|^2 e^{i\omega_{\mathbf{k}}(t-t')} [\bar{n}_2(\omega_{\mathbf{k}}, T) + 1], \end{aligned} \quad (4.11)$$

where it has been explicitly shown that both reservoirs are independent (the density operator is given by the product: $R = R_1 R_2$). In addition, we have used the commutators $[r_j, r_j^\dagger] = 1$ and $[r_{\mathbf{k}\lambda}, r_{\mathbf{k}\lambda}^\dagger] = 1$ in the last equations of (4.10) and (4.11), respectively; and introduced $\langle r_j^\dagger r_j \rangle_{R_1} = \bar{n}_1(\omega_j, T)$ and $\langle r_{\mathbf{k}\lambda}^\dagger r_{\mathbf{k}\lambda} \rangle_{R_2} = \bar{n}_2(\omega_{\mathbf{k}}, T)$, the mean number of oscillators with frequencies ω_j in \mathcal{R}_1 and $\omega_{\mathbf{k}}$ in \mathcal{R}_2 , in thermal equilibrium at temperature T , which are given by

$$\bar{n}_1(\omega_j, T) = \frac{e^{-\frac{\hbar\omega_j}{k_B T}}}{1 - e^{-\frac{\hbar\omega_j}{k_B T}}}, \quad \bar{n}_2(\omega_{\mathbf{k}}, T) = \frac{e^{-\frac{\hbar\omega_{\mathbf{k}}}{k_B T}}}{1 - e^{-\frac{\hbar\omega_{\mathbf{k}}}{k_B T}}}. \quad (4.12)$$

Furthermore, due to the reservoirs independence, the correlations involving operators from both \mathcal{R}_1 and \mathcal{R}_2 will not contribute. As an example:

$$\langle \tilde{\Gamma}_1(t) \tilde{\Gamma}_2^\dagger(t') \rangle_R = \sum_{\mathbf{k}\lambda j} \kappa_j \kappa_{\mathbf{k}\lambda}^* e^{-i(\omega_j t - \omega_{\mathbf{k}} t')} \langle r_j r_{\mathbf{k}\lambda}^\dagger \rangle_R = \sum_{\mathbf{k}\lambda j} \kappa_j \kappa_{\mathbf{k}\lambda}^* e^{-i(\omega_j t - \omega_{\mathbf{k}} t')} \langle r_j \rangle_{R_1} \langle r_{\mathbf{k}\lambda}^\dagger \rangle_{R_2} = 0. \quad (4.13)$$

With this considerations, and making the change of variable $\tau = t - t'$, the master equation (3.18) for this particular case contains 16 non-zero terms:

$$\begin{aligned} \dot{\rho} = - \int_0^t d\tau \{ & [aa^\dagger \tilde{\rho}(t-\tau) - a^\dagger \tilde{\rho}(t-\tau)a] e^{-i\omega_S \tau} \langle \tilde{\Gamma}_1^\dagger(t) \tilde{\Gamma}_1(t-\tau) \rangle_R + h.c. \\ & [a^\dagger a \tilde{\rho}(t-\tau) - a \tilde{\rho}(t-\tau) a^\dagger] e^{i\omega_S \tau} \langle \tilde{\Gamma}_1(t) \tilde{\Gamma}_1^\dagger(t-\tau) \rangle_R + h.c. \\ & [\sigma_- \sigma_+ \tilde{\rho}(t-\tau) - \sigma_+ \tilde{\rho}(t-\tau) \sigma_-] e^{-i\omega_S \tau} \langle \tilde{\Gamma}_2^\dagger(t) \tilde{\Gamma}_2(t-\tau) \rangle_R + h.c. \\ & [\sigma_+ \sigma_- \tilde{\rho}(t-\tau) - \sigma_- \tilde{\rho}(t-\tau) \sigma_+] e^{i\omega_S \tau} \langle \tilde{\Gamma}_2(t) \tilde{\Gamma}_2^\dagger(t-\tau) \rangle_R + h.c. \}. \quad (4.14) \end{aligned}$$

From now on, we will assume the difference between proximate, unlike wave vectors \mathbf{k} to be small enough to consider its spectrum as a continuum. Hence, following a similar reasoning for the frequencies ω_j , the non-vanishing reservoir correlation functions can be restated as

$$\begin{aligned} \langle \tilde{\Gamma}_1^\dagger(t) \tilde{\Gamma}_1(t-\tau) \rangle_R &= \int d\omega e^{i\omega\tau} g(\omega) |\kappa(\omega)|^2 \bar{n}_1(\omega, T), \\ \langle \tilde{\Gamma}_1(t) \tilde{\Gamma}_1^\dagger(t-\tau) \rangle_R &= \int d\omega e^{-i\omega\tau} g(\omega) |\kappa(\omega)|^2 [\bar{n}_1(\omega, T) + 1], \\ \langle \tilde{\Gamma}_2^\dagger(t) \tilde{\Gamma}_2(t-\tau) \rangle_R &= \sum_\lambda \int d^3\mathbf{k} e^{ikc\tau} g(\mathbf{k}) |\kappa(\mathbf{k}, \lambda)|^2 \bar{n}_2(kc, T), \\ \langle \tilde{\Gamma}_2(t) \tilde{\Gamma}_2^\dagger(t-\tau) \rangle_R &= \sum_\lambda \int d^3\mathbf{k} e^{-ikc\tau} g(\mathbf{k}) |\kappa(\mathbf{k}, \lambda)|^2 [\bar{n}_2(kc, T) + 1], \quad (4.15) \end{aligned}$$

where the dispersion relation $\omega = kc$ has been used to rewrite the frequency in terms of the wave vector. In addition, we have introduced the densities of states $g(\mathbf{k})$ and $g(\omega)$, defined such that $g(\mathbf{k})d^3\mathbf{k}$ and $g(\omega)d\omega$ account for the number of photons with wave vectors in the interval $[\mathbf{k}, \mathbf{k} + d^3\mathbf{k}]$, and the number of oscillators from \mathcal{R}_1 with frequencies in $[\omega, \omega + d\omega]$, respectively. In the Markoff approximation, we consider $\tau \ll t$, where τ is the reservoir correlation time and t the time scale for changes in ρ . Therefore, we can do the replacement $\tilde{\rho}(t-\tau) \simeq \tilde{\rho}(t) \equiv \tilde{\rho}$ and, since the τ integration is dominated by short times due to the exponential term, we can extend the integrals to infinity:

$$\begin{aligned} \lim_{t \rightarrow \infty} \int_0^t d\tau e^{-i(\omega - \omega_S)\tau} &= \pi \delta(\omega - \omega_S) + i \frac{P}{\omega_S - \omega}, \\ \lim_{t \rightarrow \infty} \int_0^t d\tau e^{-i(kc - \omega_S)\tau} &= \pi \delta(kc - \omega_S) + i \frac{P}{\omega_S - kc}, \quad (4.16) \end{aligned}$$

where P refers to the Cauchy principal value. Therefore, introducing

$$\begin{aligned}\kappa_1 &= \pi g(\omega_S) |\kappa(\omega_S)|^2, & \kappa_2 &= \pi \sum_{\lambda} \int d^3\mathbf{k} g(\mathbf{k}) |\kappa(\mathbf{k}, \lambda)|^2 \delta(kc - \omega_S), \\ \Delta_1 &= P \int_0^{\infty} d\omega \frac{g(\omega) |\kappa(\omega)|^2}{\omega_S - \omega}, & \Delta_2 &= \sum_{\lambda} P \int d^3\mathbf{k} \frac{g(\mathbf{k}) |\kappa(\mathbf{k}, \lambda)|^2}{\omega_S - kc}, \\ \Delta'_1 &= P \int_0^{\infty} d\omega \frac{g(\omega) |\kappa(\omega)|^2}{\omega_S - \omega} \bar{n}_1(\omega, T), & \Delta'_2 &= \sum_{\lambda} P \int d^3\mathbf{k} \frac{g(\mathbf{k}) |\kappa(\mathbf{k}, \lambda)|^2}{\omega_S - kc} \bar{n}_2(kc, T),\end{aligned}\tag{4.17}$$

the terms related to each subsystem \mathcal{S}_p can be written as

$$\int d\tau e^{-i\omega_S \tau} \langle \tilde{\Gamma}_p^\dagger(t) \tilde{\Gamma}_p(t - \tau) \rangle_R \simeq \kappa_p \bar{n}_p + i\Delta'_p, \quad \int d\tau e^{-i\omega_S \tau} \langle \tilde{\Gamma}_p(t) \tilde{\Gamma}_p^\dagger(t - \tau) \rangle_R \simeq \kappa_p (1 + \bar{n}_p) + i\Delta_p + i\Delta'_p,\tag{4.18}$$

where we have set $\bar{n}_1 \equiv \bar{n}_1(\omega_S, T)$ and $\bar{n}_2 \equiv \bar{n}_2(\omega_S, T)$. Substituting the previous result in the master equation (4.14) we obtain

$$\begin{aligned}\dot{\tilde{\rho}} &= (\kappa_1 + i\Delta_1)(a\tilde{\rho}a^\dagger - a^\dagger a\tilde{\rho}) + \text{h.c.} + (\kappa_2 + i\Delta_2)(\sigma_- \tilde{\rho} \sigma_+ - \sigma_+ \sigma_- \tilde{\rho}) + \text{h.c.} \\ &+ (\kappa_1 \bar{n}_1 + i\Delta'_1)(a\tilde{\rho}a^\dagger - a^\dagger a\tilde{\rho} + a^\dagger \tilde{\rho} a - \tilde{\rho} a a^\dagger) + \text{h.c.} \\ &+ (\kappa_2 \bar{n}_2 + i\Delta'_2)(\sigma_- \tilde{\rho} \sigma_+ - \sigma_+ \sigma_- \tilde{\rho} + \sigma_+ \tilde{\rho} \sigma_- - \tilde{\rho} \sigma_- \sigma_+) + \text{h.c.}\end{aligned}\tag{4.19}$$

We will now calculate a simpler formula. Expanding the terms associated to \mathcal{S}_1 :

$$\begin{aligned}i) \quad & \kappa_1 (a\tilde{\rho}a^\dagger - a^\dagger a\tilde{\rho} + a\tilde{\rho}a^\dagger - \tilde{\rho}a^\dagger a) = \kappa_1 (2a\tilde{\rho}a^\dagger - a^\dagger a\tilde{\rho} - \tilde{\rho}a^\dagger a), \\ ii) \quad & i\Delta_1 (a\tilde{\rho}a^\dagger - a^\dagger a\tilde{\rho} - a\tilde{\rho}a^\dagger + \tilde{\rho}a^\dagger a) = -i\Delta_1 [a^\dagger a, \tilde{\rho}], \\ iii) \quad & \kappa_1 \bar{n}_1 (a\tilde{\rho}a^\dagger - a^\dagger a\tilde{\rho} + a^\dagger \tilde{\rho} a - \tilde{\rho} a a^\dagger + a\tilde{\rho}a^\dagger - \tilde{\rho}a^\dagger a + a^\dagger \tilde{\rho} a - a a^\dagger \tilde{\rho}) = \\ & \kappa_1 \bar{n}_1 (2a\tilde{\rho}a^\dagger + 2a^\dagger \tilde{\rho} a - (2a^\dagger a + 1)\tilde{\rho} - \tilde{\rho}(2aa^\dagger - 1)) = 2\kappa_1 \bar{n}_1 (a\tilde{\rho}a^\dagger + a^\dagger \tilde{\rho} a - a^\dagger a\tilde{\rho} - \tilde{\rho} a a^\dagger), \\ iv) \quad & i\Delta'_1 (a\tilde{\rho}a^\dagger - a^\dagger a\tilde{\rho} + a^\dagger \tilde{\rho} a - \tilde{\rho} a a^\dagger - a\tilde{\rho}a^\dagger + \tilde{\rho}a^\dagger a - a^\dagger \tilde{\rho} a + a a^\dagger \tilde{\rho}) = \\ & i\Delta'_1 (-\tilde{\rho}[a, a^\dagger] + [a, a^\dagger]\tilde{\rho}) = 0.\end{aligned}\tag{4.20}$$

For \mathcal{S}_2 we get a similar first term, but replacing $a, a^\dagger \rightarrow \sigma_-, \sigma_+$. To obtain the others, we must introduce some properties of the σ operators:

$$\begin{aligned}\sigma_z &= |e\rangle\langle e| - |g\rangle\langle g|, & \sigma_- &= |g\rangle\langle e|, & \sigma_+ &= |e\rangle\langle g|, \\ \sigma_\pm \sigma_\mp &= \frac{1}{2}(\mathbb{1}_{S_2} \pm \sigma_z), & \{\sigma_+, \sigma_-\} &= \mathbb{1}_{S_2}, & [\sigma_+, \sigma_-] &= \sigma_z.\end{aligned}\tag{4.21}$$

Thus,

$$\begin{aligned}ii) \quad & i\Delta_2 (\sigma_- \tilde{\rho} \sigma_+ - \sigma_+ \sigma_- \tilde{\rho} - \sigma_- \tilde{\rho} \sigma_+ + \tilde{\rho} \sigma_+ \sigma_-) = -i\Delta_2 [\sigma_+ \sigma_-, \tilde{\rho}] = -\frac{i}{2} \Delta_2 [\sigma_z, \tilde{\rho}], \\ iii) \quad & \kappa_2 \bar{n}_2 (2\sigma_- \tilde{\rho} \sigma_+ + 2\sigma_+ \tilde{\rho} \sigma_- - \tilde{\rho} \{\sigma_-, \sigma_+\} - \{\sigma_-, \sigma_+\} \tilde{\rho}) = 2\kappa_2 \bar{n}_2 (\sigma_- \tilde{\rho} \sigma_+ + \sigma_+ \tilde{\rho} \sigma_- - \tilde{\rho}), \\ iv) \quad & -i\Delta'_2 ([\sigma_+, \sigma_-] \tilde{\rho} - \tilde{\rho} [\sigma_+, \sigma_-]) = -i\Delta'_2 [\sigma_z, \tilde{\rho}].\end{aligned}\tag{4.22}$$

Substituting these results in (4.19) we obtain

$$\begin{aligned} \dot{\tilde{\rho}} = & -i\Delta_1[a^\dagger a, \tilde{\rho}] + \kappa_1(2a\tilde{\rho}a^\dagger - a^\dagger a\tilde{\rho} - \tilde{\rho}a^\dagger a) + 2\kappa_1\bar{n}_1(a\tilde{\rho}a^\dagger + a^\dagger\tilde{\rho}a - a^\dagger a\tilde{\rho} - \tilde{\rho}aa^\dagger) \\ & - \frac{i}{2}(\Delta_2 + 2\Delta'_2)[\sigma_z, \tilde{\rho}] + \kappa_2(2\sigma_- \tilde{\rho} \sigma_+ - \sigma_+ \sigma_- \tilde{\rho} - \tilde{\rho} \sigma_+ \sigma_-) + 2\kappa_2\bar{n}_2(\sigma_- \tilde{\rho} \sigma_+ + \sigma_+ \tilde{\rho} \sigma_- - \tilde{\rho}). \end{aligned} \quad (4.23)$$

We should now transform back to the Schrödinger picture:

$$\dot{\rho} = \frac{1}{i\hbar}[H_S, \rho] + e^{-\frac{i}{\hbar}(H_{S_1}+H_{S_2})t} \dot{\tilde{\rho}} e^{\frac{i}{\hbar}(H_{S_1}+H_{S_2})t}, \quad H_S = H_{S_1} + H_{S_2} + H_{JC}. \quad (4.24)$$

Consequently, we obtain the master equation

$$\begin{aligned} \dot{\rho} = & -i\omega'_c[a^\dagger a, \rho] + \kappa_1(2a\rho a^\dagger - a^\dagger a\rho - \rho a^\dagger a) + 2\kappa_1\bar{n}_1(a\rho a^\dagger + a^\dagger\rho a - a^\dagger a\rho - \rho a a^\dagger) \\ & - \frac{i}{2}\omega'_A[\sigma_z, \rho] + \kappa_2(2\sigma_- \rho \sigma_+ - \sigma_+ \sigma_- \rho - \rho \sigma_+ \sigma_-) + 2\kappa_2\bar{n}_2(\sigma_- \rho \sigma_+ + \sigma_+ \rho \sigma_- - \rho) \\ & - id[a^\dagger \sigma_-, \rho] - id^*[a\sigma_+, \rho], \end{aligned} \quad (4.25)$$

where

$$\omega'_c = \omega_S + \Delta_1, \quad \omega'_A = \omega_S + \Delta_2 + 2\Delta'_2. \quad (4.26)$$

Thereby, (4.25) is the master equation in the Born-Markoff approximation for a harmonic oscillator and a two-state atom that influence each other via a Jaynes-Cummings interaction, when they are affected by a single, separate reservoir and both reservoirs are a collection of harmonic oscillators. We can now calculate the matrix elements of $\dot{\rho}$ by projecting it onto the eigenstates of $\mathcal{S} = \mathcal{S}_1 \oplus \mathcal{S}_2$. Since \mathcal{H}_{S_1} and \mathcal{H}_{S_2} are independent, they will be given by the tensor product of the eigenstates of each subsystem: the $|n\rangle \otimes |g\rangle$ and $|n\rangle \otimes |e\rangle$ states. Hence,

$$\begin{aligned} \dot{\rho}_{mfnh} = & -[i\omega'_c(m-n) + \kappa_1(m+n+2\bar{n}_1(m+n+1))] \rho_{mfnh} + 2\kappa_1\bar{n}_1\sqrt{mn}\rho_{m-1,f,n-1,h} \\ & + 2\kappa_1\sqrt{(m+1)(n+1)(\bar{n}_1+1)}\rho_{m+1,f,n+1,h} + 2\kappa_2(\bar{n}_2+1)\rho_{m,f+1,n,h+1} \\ & - [i\omega'_A(\delta_{f1}\delta_{h0} - \delta_{f0}\delta_{h1}) + \kappa_2(2\bar{n}_2 + \delta_{f1} + \delta_{h1})] \rho_{mfnh} + 2\kappa_2\bar{n}_2\rho_{m,f-1,n,h-1} \\ & - id\sqrt{m}\rho_{m-1,f+1,nh} + id\sqrt{n+1}\rho_{mf,n+1,h-1} \\ & - id^*\sqrt{m+1}\rho_{m+1,f-1,nh} + id^*\sqrt{n}\rho_{mf,n-1,h+1}, \end{aligned} \quad (4.27)$$

where $\dot{\rho}_{mfnh} \equiv \langle m, f | \dot{\rho} | n, h \rangle$. Regarding the harmonic oscillator \mathcal{S}_1 , the requirement $n, m \geq 0$ must be fulfilled; and with respect to the two-state atom \mathcal{S}_2 we have the condition $f, h \in \{0, 1\}$, corresponding to the states $|g\rangle$ and $|e\rangle$, respectively. We see that the first three terms account for the interaction between \mathcal{S}_1 and \mathcal{R}_1 , the following three are the equivalent (with different order) for \mathcal{S}_2 and \mathcal{R}_2 ; and the last four correspond to the Jaynes-Cumming's interaction between \mathcal{S}_1 and \mathcal{S}_2 . Regarding the populations ($n = m$, $f = h$), we can identify the transitions shown in Table 1.

Transitions	Transition rates
$ n+1, f\rangle \rightarrow n, f\rangle$	$2\kappa_1(n+1)(\bar{n}_1+1)$
$ n-1, f\rangle \rightarrow n, f\rangle$	$2\kappa_1\bar{n}_1n$
$ n, f\rangle \rightarrow n-1, f\rangle$	$2\kappa_1n(\bar{n}_1+1)$
$ n, f\rangle \rightarrow n+1, f\rangle$	$2\kappa_1\bar{n}_1(n+1)$
$ n, e\rangle \rightarrow n, g\rangle$	$2\kappa_2(\bar{n}_2+1)$
$ n, g\rangle \rightarrow n, e\rangle$	$2\kappa_2\bar{n}_2$

Table 1: Possible transitions and transition rates

Without taking into account the interaction between \mathcal{S}_1 and \mathcal{S}_2 , we see that when $T = 0\text{K}$ ($\bar{n}_i = 0$), all transition rates from lower-energy levels vanish, while for the transitions from higher-energy levels there are non-zero contributions, identified as spontaneous emission rates. This process, where each subsystem leaks a photon or phonon, depending on the type of interaction, to their respective reservoir; would ultimately produce the decay to the ground state for the $T = 0\text{K}$ case. On the other hand, when $T \neq 0\text{K}$ we see that transitions to higher levels are allowed, where the system increases its energy by the absorption of any of the mentioned particles of the reservoirs, in a process named induced absorption.

With respect to the JC interaction, due to its operators $a\sigma_+$ and $a^\dagger\sigma_-$, it will only connect the $|n+1, g\rangle$ and $|n, e\rangle$ states. The relevant terms of the matrix element evolution for each of those levels are

$$\begin{aligned}
\dot{\rho}_{nene} &= \dots + id\sqrt{n+1}\rho_{n+1,g,ne} - id^*\sqrt{n+1}\rho_{n+1g,n,e} = \dots + 2i\text{Re}\{d\}\sqrt{n+1}\rho_{ne,n+1,g}, \\
\dot{\rho}_{n+1,g,n+1,g} &= \dots - 2i\text{Re}\{d\}\sqrt{n+1}\rho_{ne,n+1,g}, \\
\dot{\rho}_{ne,n+1,g} &= \dots - id^*\sqrt{n+1}(\rho_{n+1,g,n+1,g} - \rho_{nene}).
\end{aligned} \tag{4.28}$$

Therefore, an unevenness in the populations generates coherences that will later contribute to restore the equilibrium, which can be reached or not. It can also be seen that when the term proportional to d dominates, the sign of d does not affect the evolution of the populations, due to the generation of opposite sign coherences. Furthermore, since $\dot{\rho}_{n+1,g,n+1,g}$ depends on $\rho_{ne,n+1,g}$ and not on its evolution, the transfer of populations due to the imbalance will have some delay. In the case of \mathcal{S} being isolated from the environment ($\kappa_1 = \kappa_2 = 0$) and in a state $|\Psi\rangle = c_1(t)|n+1, g\rangle + c_2(t)|n, e\rangle$, according to (4.28) we would have $\dot{c}_1 = -c_2$ and vice versa, which corresponds to Rabi oscillations.

4.2 Stationary states

The goal is to calculate the stationary states for the ensemble $\mathcal{S} = \mathcal{S}_1 \oplus \mathcal{S}_2$. The populations of such states must verify $\dot{\rho}_{nfnf} = 0$, an equation that involves the coherence $\rho_{ne,n+1,g}$ and the populations of many other states; in fact indirectly infinitely many due

to the mentioned coherence, as we should show. From (4.27) we find that in the stationary limit

$$\begin{aligned} \rho_{ne,n+1,g} = f & \left(\rho_{nene}, \rho_{n+1,g,n+1,g}, \right. \\ & \rho_{n-1,e,ng} \left(\rho_{n-1,e,n-1,e}, \rho_{ngng}, \rho_{ne,n+1,g}(\dots), \rho_{n-2,e,n-1,g}(\dots) \right), \\ & \left. \rho_{n+1,e,n+2,g} \left(\rho_{n+1,e,n+1,e}, \rho_{n+2,g,n+2,g}, \rho_{ne,n+1,g}(\dots), \rho_{n+2,e,n+3,g}(\dots) \right) \right). \end{aligned} \quad (4.29)$$

Hence, in order to calculate an approximate result, a different approach will be followed. During the derivation of the master equation, it was stated that both reservoirs were independent, which led to equation (4.14). The direct consequence is the separation of each $\mathcal{S}_i - \mathcal{R}_i$ interaction, which allows us to associate the terms in the first and second line of (4.25) to the ones we would have obtained if calculated the master equation for a harmonic oscillator or a two-state atom, respectively. More explicitly, the matrix elements would be given by

$$\begin{aligned} \dot{\rho}_{mn} = & - [i\omega'_c(m-n) + \kappa_1(m+n+2\bar{n}_1(m+n+1))] \rho_{mn} + 2\kappa_1\bar{n}_1\sqrt{m\bar{n}}\rho_{m-1,n-1}, \\ & + 2\kappa_1\sqrt{(m+1)(n+1)}(\bar{n}_1+1)\rho_{m+1,n+1}, \end{aligned} \quad (4.30)$$

$$\begin{aligned} \dot{\rho}_{fh} = & - [i\omega'_A(\delta_{f1}\delta_{h0} - \delta_{f0}\delta_{h1}) + \kappa_2(2\bar{n}_2 + \delta_{f1} + \delta_{h1})] \rho_{fh} + 2\kappa_2\bar{n}_2\rho_{f-1,h-1} \\ & + 2\kappa_2(\bar{n}_2+1)\rho_{f+1,h+1}. \end{aligned} \quad (4.31)$$

We can easily calculate the stationary states for the two-state atom case:

$$\dot{\rho}_{gg} = 0 = 2\kappa_2[-\bar{n}_2\rho_{gg} + (\bar{n}_2+1)\rho_{ee}] \implies -\bar{n}_2\rho_{gg} + (\bar{n}_2+1)(1-\rho_{gg}) = 0, \quad (4.32)$$

where we have used $\text{Tr } \rho = \rho_{gg} + \rho_{ee} = 1$. Thus,

$$\rho_{gg}(t \rightarrow \infty) = \frac{\bar{n}_2+1}{2\bar{n}_2+1}, \quad \rho_{ee}(t \rightarrow \infty) = \frac{\bar{n}_2}{2\bar{n}_2+1}. \quad (4.33)$$

In the case of the harmonic oscillator, we will use a recurrence procedure, ultimately writing each population² in terms of the ground state:

$$\begin{aligned} \dot{\rho}_{00} = 0 = -2\kappa_1[\bar{n}_1\rho_{00} - (\bar{n}_1+1)\rho_{11}] & \implies \rho_{11} = \frac{\bar{n}_1}{\bar{n}_1+1}\rho_{00}, \\ \dot{\rho}_{11} = 0 = -2\kappa_1[(1+3\bar{n}_1)\rho_{11} - \bar{n}_1\rho_{00} - 2(\bar{n}_1+1)\rho_{22}] & \implies \rho_{22} = \frac{\bar{n}_1^2}{(\bar{n}_1+1)^2}\rho_{00}. \end{aligned} \quad (4.34)$$

We see the emergence of the pattern

$$\rho_{nn} = \left(\frac{\bar{n}_1}{\bar{n}_1+1} \right)^n \rho_{00}. \quad (4.35)$$

Then, using the trace of ρ we can determine ρ_{00} :

$$\text{Tr } \rho = 1 = \sum_{n=0}^{\infty} \left(\frac{\bar{n}_1}{\bar{n}_1+1} \right)^n \rho_{00} = \rho_{00} \frac{1}{1 - \frac{\bar{n}_1}{\bar{n}_1+1}} = \rho_{00}(\bar{n}_1+1) \implies \rho_{00} = \frac{1}{\bar{n}_1+1}, \quad (4.36)$$

²To lighten the notation, we will not write the $t \rightarrow \infty$ limit.

which substituted back in (4.35) gives

$$\rho_{nn}(t \rightarrow \infty) = \frac{\bar{n}_1^n}{(\bar{n}_1 + 1)^{n+1}}. \quad (4.37)$$

From the previous equation and (4.33) it can be seen that in those cases the stationary limit only depends in the state of the reservoirs (the \bar{n}_i); which allows us to conclude that the coupling constants κ_i exclusively affect the transition rates and hence the time needed to reach the final state. Considering now the composite system, if we neglect the JC interaction ($d \rightarrow 0$), both subsystems will evolve independently. Thereby, each $\mathcal{S}_i - \mathcal{R}_i$ interaction will set the final state of the respective subsystem, and we can calculate the populations as

$$\rho_{nfnf} = \mathcal{P}(|n, f\rangle) = \mathcal{P}(|n\rangle)\mathcal{P}(|f\rangle) = \frac{\bar{n}_1^n}{(\bar{n}_1 + 1)^{n+1}} \frac{\bar{n}_2 + 1 - f}{2\bar{n}_2 + 1}. \quad (4.38)$$

Therefore, the last result can be considered as a zeroth-order approximation in d for the populations in the stationary limit, valid in the $d \ll 1$ case. When the JC interaction is strong we can qualitatively explain the behaviour of the system. In the preceding section, specifically in equation (4.28), it was shown that the $\mathcal{S}_1\mathcal{S}_2$ coupling modifies the populations to counterbalance the difference between the $|ne\rangle$ and $|n+1, g\rangle$ states, which can be approximated to

$$\rho_{nene} - \rho_{n+1,g,n+1,g} = \frac{\bar{n}_1^n}{(\bar{n}_1 + 1)^{n+2}(2\bar{n}_2 + 1)} (\bar{n}_2 - \bar{n}_1) + \mathcal{O}(d). \quad (4.39)$$

Thus, if $\bar{n}_1 < \bar{n}_2$ we would expect the correction to lower ρ_{nene} and rise $\rho_{n+1,g,n+1,g}$ and vice versa if $\bar{n}_1 > \bar{n}_2$. In the $\bar{n}_2 = \bar{n}_1$ case we should thereby predict a negligible correction.

4.3 Numerical solution

We will calculate the evolution of the density matrix elements for two different cases:

- I) An initial state $|\Psi(0)\rangle = |2, e\rangle$, with parameters $\omega'_A = \omega'_c = 3\omega_0$, $\kappa_1 = \kappa_2 = d = 1.4\omega_0$ and $\bar{n}_1 = \bar{n}_2 = 0$.
- II) An initial state $|\Psi(0)\rangle = 1/\sqrt{14}(3|2, e\rangle + |2, g\rangle + 2|1, e\rangle)$ and parameters: $\omega'_A = \omega'_c = 3\omega_0$, $\kappa_1 = \kappa_2 = d = 1.4\omega_0$, $\bar{n}_1 = 0.5$ and $\bar{n}_2 = 1$. We will consider also the cases $\bar{n}_1 = \bar{n}_2 = 1$, and $\bar{n}_1 = 1$ and $\bar{n}_2 = 0.5$.

There are two main differences between both situations:

- Temperature. In (I) we have $\bar{n}_i = 0$, which implies $T = 0\text{K}$ for both reservoirs, while (II) corresponds to the opposite case.
- Initial coherences. Only (II) has non-null initial values for some coherences, as the initial state is a linear combination of states. Furthermore, due to the fact that it can not be written as a tensor product of states of each subsystem, $|\Psi(0)\rangle$ (II) is an entangled state.

Since we are only interested in the behaviour of the system, no specific units will be used for the parameters. For this reason, we have introduced ω_0 , an arbitrary frequency unit such that $\omega_0 t$ is dimensionless.

4.3.1 Pure state at T=0K

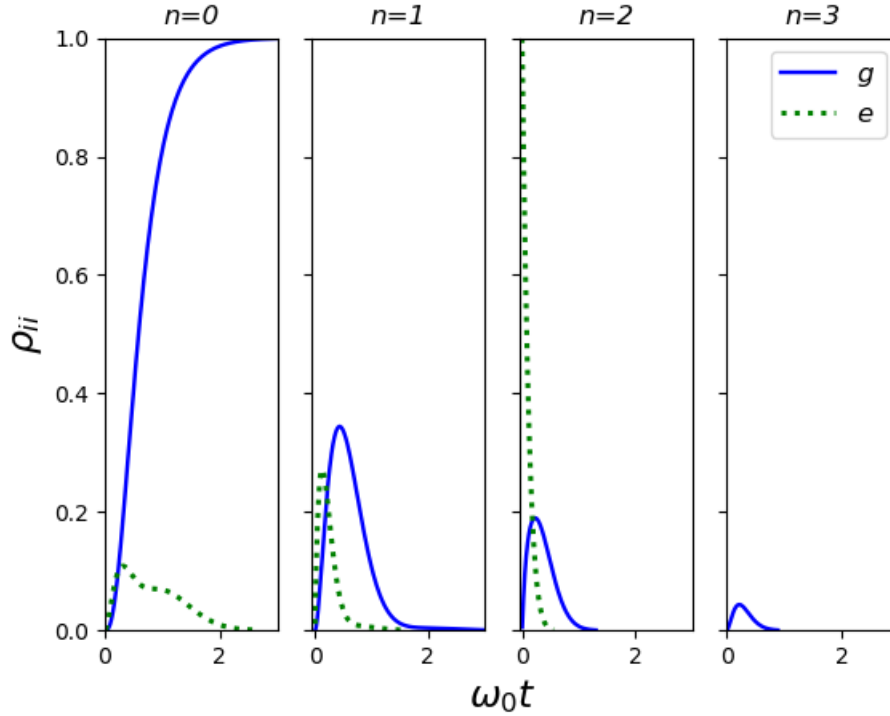


Figure 1: Evolution of populations for case (I): initial state $|\Psi(0)\rangle = |2, e\rangle$, with $\omega'_A = \omega'_c = 3\omega_0$, $\kappa_1 = \kappa_2 = d = 1.4\omega_0$ and $\bar{n}_1 = \bar{n}_2 = 0$. Those corresponding to \mathcal{S}_2 being in the ground state are plotted using solid lines, and for its the excited state dashed lines are used.

As we can see in Figure 1, populations progressively decay to lower-energy states, eventually reaching $\mathcal{P}(|0, g\rangle) = \rho_{0g0g} = 1$. Therefore, in this case the decoherence would imply dissipation. Since we are considering $T = 0K$, the observed evolution can be explained by the spontaneous emission terms mentioned before. However, there are also transitions to higher-energy levels due to the Jaynes-Cumming's Hamiltonian, which connects the levels $|n, e\rangle - |n + 1, g\rangle$ and vice versa; and we can see the isolated effect of this interaction in the initial rise of the $|3, g\rangle$ populations. Furthermore, it can be noticed that the $|n, e\rangle$ states rise and decay faster than the $|n, g\rangle$ states. As we have chosen the coupling constants to be equal and transition rates for each subsystem are similar for small n values, this behaviour can be explained by the possible transitions available.

The fact that $|2, e\rangle$ is the initial state, implies that $|1, e\rangle$ can directly get populations, while $|1, g\rangle$ needs first $|2, g\rangle$ populations to grow. This pattern, displayed in Figure 2, explains the faster rise of the $|n, e\rangle$ states; and their quicker decay is related to the amount of

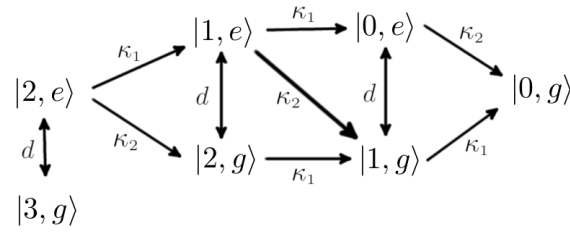


Figure 2: Transition scheme for case (I): initial state $|\Psi(0)\rangle = |2, e\rangle$, with $\omega'_A = \omega'_c = 3\omega_0$, $\kappa_1 = \kappa_2 = d = 1.4\omega_0$ and $\bar{n}_1 = \bar{n}_2 = 0$. The directionality of the transition is shown by the arrows, and the interaction that causes it is represented by its coupling constant: $H_{S_i\mathcal{R}_i}(\kappa_i)$ and $H_{JC}(d)$.

levels each state can decay to. In general, $|n, e\rangle$ can transfer populations to $|n + 1, g\rangle$, $|n, g\rangle$ or $|n - 1, e\rangle$, while $|n, g\rangle$ only to $|n - 1, g\rangle$ and $|n - 1, e\rangle$.

In Figure 1 it is shown the transition from a pure state $|2, e\rangle$ to a mixed one, to eventually become a pure state again ($|0, g\rangle$). We can justify this evolution by studying the Von Neumann entropy and the trace of ρ^2 , which verify

$$S_{\mathcal{V}\mathcal{N}} = -\text{Tr} \rho \ln \rho \geq 0, \quad \text{Tr} \rho^2 \leq 1, \quad (4.40)$$

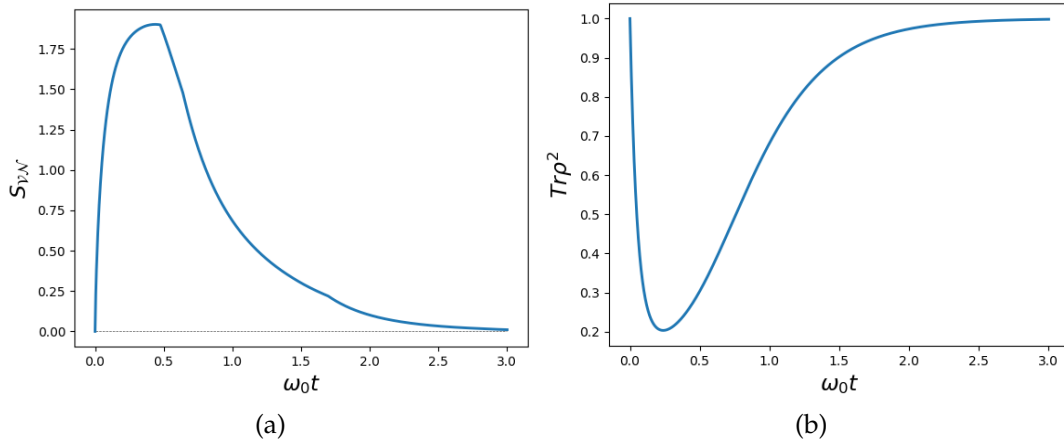


Figure 3: Evolution of $S_{\mathcal{V}\mathcal{N}}$ (a) and $\text{Tr} \rho^2$ (b) for case (I): initial state $|\Psi(0)\rangle = |2, e\rangle$, with $\omega'_A = \omega'_c = 3\omega_0$, $\kappa_1 = \kappa_2 = d = 1.4\omega_0$ and $\bar{n}_1 = \bar{n}_2 = 0$.

where the equalities are fulfilled only for pure states. According to Figure 3, both have an extremum at $\omega_0 t = 0.26$, which is the time where the populations are more evenly distributed (highest average and lowest standard deviation). As the second law of Thermodynamics states that $\Delta S \geq 0$ in a closed system, the entropy of the total system should increase or stay the same. Thereby, the decrease seen in the entropy of S must entail an increase in the entropy of the reservoir set \mathcal{R} .

Regarding coherences, the only non-null values correspond to the $|n, g\rangle - |n-1, e\rangle$ matrix elements, the ones affected by the JC interaction. As d was chosen to be real, only imaginary coherences were obtained; allowing us to obtain information from their inflection points more accurately.

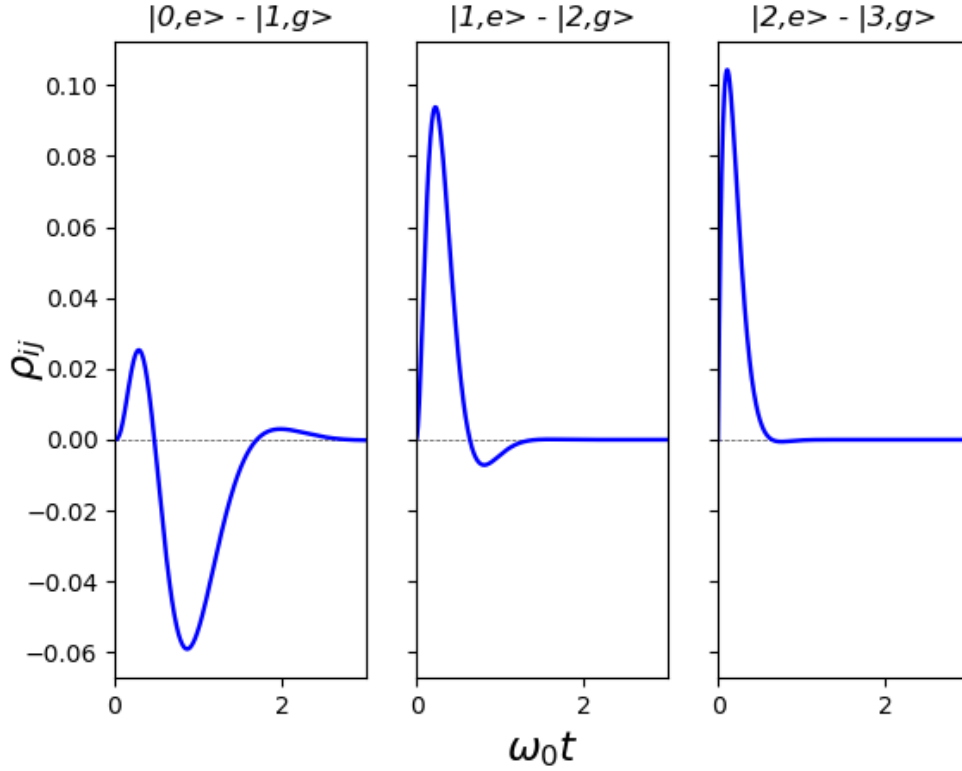


Figure 4: Evolution of coherences (imaginary part) for case (I): initial state $|\Psi(0)\rangle = |2, e\rangle$, with $\omega'_A = \omega'_c = 3\omega_0$, $\kappa_1 = \kappa_2 = d = 1.4\omega_0$ and $\bar{n}_1 = \bar{n}_2 = 0$.

Taking into account both (4.28) and Figure 1, the inflection points can be approximately associated to those where there is a flip in the relation between populations:

$$\rho_{ngng} > \rho_{n-1,e,n-1,e} \longleftrightarrow \rho_{ngng} < \rho_{n-1,e,n-1,e}. \quad (4.41)$$

However, writing down the full expression for the matrix element evolution of the relevant coherence that influences this transition, for the case where $d \in \mathfrak{R}$ and $\omega'_A = \omega'_c$:

$$\begin{aligned} \dot{\rho}_{ne,n+1,g} = & - \left[\kappa_1 (2n + 1 + 4\bar{n}_1(n + 1)) + \kappa_2 (2\bar{n}_2 + 1) \right] \rho_{ne,n+1,g} \\ & + 2\kappa_1 \bar{n}_1 \sqrt{n(n + 1)} \rho_{n-1,e,ng} + 2\kappa_1 (\bar{n}_1 + 1) \sqrt{(n + 2)(n + 1)} \rho_{n+1,e,n+2,g} \\ & - id\sqrt{n + 1} (\rho_{n+1,g,n+1,g} - \rho_{nene}), \end{aligned} \quad (4.42)$$

we see that $\rho_{ne,n+1,g}$ is affected by the presence of coherences of the $\{|n + 1, g\rangle, |ne\rangle\}$ subset of states, also involved in the JC interaction; and for $\bar{n}_1 \neq 0$ would also be affected by those from the $\{|ng\rangle, |n - 1, e\rangle\}$ pair. Interestingly, we see that the $\mathcal{R}_2 - \mathcal{S}_2$ coupling

only accelerates the rate of coherence loss, due to the restriction of \mathcal{S}_2 only having two energy levels ($f, h \in \{0, 1\}$). Regarding Figure 4, the last two graphs can be explained by the flipping argument alone. As an example, until $\omega_0 t \approx 0.2$, $\mathcal{P}(|1, e\rangle) > \mathcal{P}(|2, g\rangle)$; and the opposite relation is verified afterwards. However, the first graph shows two extrema despite the fact that $\mathcal{P}(|0, e\rangle) < \mathcal{P}(|1, g\rangle)$ until $\omega_0 t = 0.9$, where the second one takes place. Therefore, the initial rise is related to the presence of positive $\rho_{1e,2g}$ coherences, which ends when the flipping term becomes dominant. As a conclusion, Figure 4 shows that when $T = 0\text{K}$, the interaction with the reservoirs produce a complete loss of the coherences. This is caused by the fact that the only interaction that generates them is H_{JC} , whose related coherences disappear when the populations of states other than $|0, g\rangle$ vanish, as seen in (4.42).

4.3.2 Entangled state at $T \neq 0\text{K}$

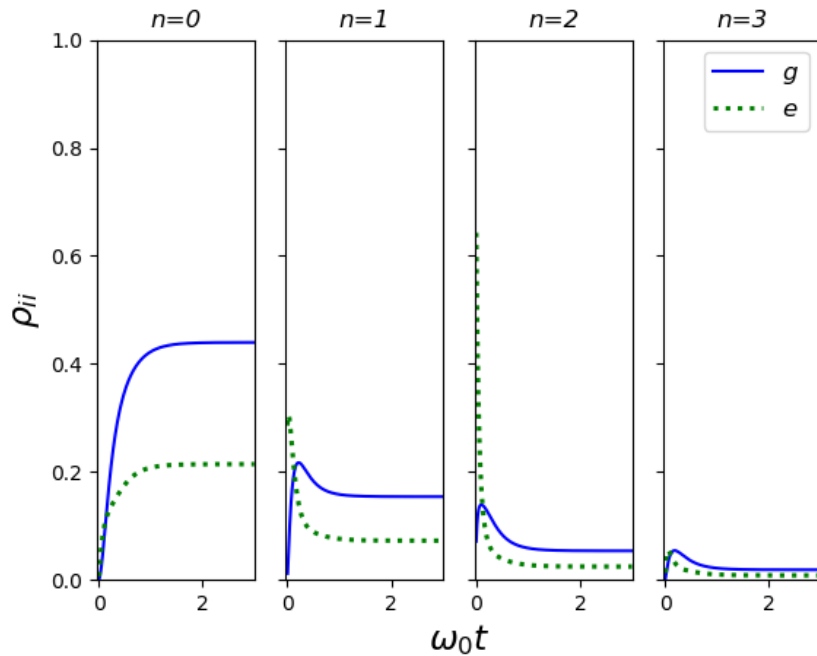


Figure 5: Evolution of populations for case (II): initial state $|\Psi(0)\rangle = 1/\sqrt{14}(3|2, e\rangle + |2, g\rangle + 2|1, e\rangle)$ with $\omega'_A = \omega'_c = 3\omega_0$, $\kappa_1 = \kappa_2 = d = 1.4\omega_0$, $\bar{n}_1 = 0.5$ and $\bar{n}_2 = 1$. Those corresponding to \mathcal{S}_2 being in the ground state are plotted using solid lines, and for its the excited state dashed lines are used.

In this case, the populations (Figure 5) eventually reach a stationary state always different than zero; having lower values for higher n states and, within the same n , greater probabilities for the $|n, g\rangle$ over the $|n, e\rangle$ states, due to the values of \bar{n}_i chosen. It is important to remark that even though only the populations of a few states have been plotted, when $\bar{n}_1 \neq 0 (T_1 \neq 0)$ all the states become populated according to equation (4.38), plus

the respective correction due to the JC interaction. We will now compare the populations with the ones we would obtain from equation (4.38), as well as with the ones numerically calculated for case(II) when $\bar{n}_1 = \bar{n}_2 = 1$ and when we set $\bar{n}_1 = 1$ and $\bar{n}_2 = 0.5$.

State	0 th order	\mathcal{P}	State	0 th order	\mathcal{P}	State	0 th order	\mathcal{P}
$ 0g\rangle$	0.4444	0.4397	$ 0g\rangle$	0.3750	0.3761	$ 0g\rangle$	0.3333	0.3327
$ 0e\rangle$	0.2222	0.2142	$ 0e\rangle$	0.1250	0.1342	$ 0e\rangle$	0.1666	0.1663
$ 1g\rangle$	0.1481	0.1540	$ 1g\rangle$	0.1875	0.1813	$ 1g\rangle$	0.1666	0.1663
$ 1e\rangle$	0.0740	0.0725	$ 1e\rangle$	0.0625	0.0676	$ 1e\rangle$	0.0833	0.0831
$ 2g\rangle$	0.0493	0.0537	$ 2g\rangle$	0.0937	0.0876	$ 2g\rangle$	0.0833	0.0831
$ 2e\rangle$	0.0246	0.0245	$ 2e\rangle$	0.0312	0.0340	$ 2e\rangle$	0.0416	0.0415
$ 3g\rangle$	0.0164	0.0186	$ 3g\rangle$	0.0468	0.0424	$ 3g\rangle$	0.0416	0.0415
$ 3e\rangle$	0.0082	0.0083	$ 3e\rangle$	0.0156	0.0170	$ 3e\rangle$	0.0208	0.0207
$ 4g\rangle$	0.0054	0.0064	$ 4g\rangle$	0.0234	0.0206	$ 4g\rangle$	0.0208	0.0207
$ 4e\rangle$	0.0027	0.0028	$ 4e\rangle$	0.0078	0.0085	$ 4e\rangle$	0.0104	0.0103

(a) $\bar{n}_1 < \bar{n}_2$ (b) $\bar{n}_1 > \bar{n}_2$ (c) $\bar{n}_2 = \bar{n}_1$

Table 2: Corrections to the populations for different values of (\bar{n}_1, \bar{n}_2) for case (II): (0.5, 1) in (a), (1, 0.5) in (b) and (1, 1) in (c).

As we see in Table 2, the JC interaction behaves differently for distinct combinations of the \bar{n}_i , according to equation (4.39). When $\bar{n}_1 = \bar{n}_2$, populations of the $\{|ne\rangle, |n+1, g\rangle\}$ states are equal in the zeroth-order approximation and, since the perturbation tends to equalize them, no significant changes are produced. Nevertheless, in the $\bar{n}_1 > \bar{n}_2$ case the $|n+1, g\rangle$ have greater populations compared to the $|n, e\rangle$ states, causing a transfer from the first to the latter; while when $\bar{n}_1 < \bar{n}_2$ we have approximately the opposite situation. It is also remarkable that even though the ground state is not directly involved in the JC interaction, its population becomes altered due to the changes in ρ_{0e0e} and ρ_{1g1g} .

As it was exposed before, it is possible to see the transition from a pure to a mixed state by analyzing the entropy and the trace of ρ^2 , shown in Figure 6. On this occasion, the system stays in a mixed state according to (4.40); and since the total entropy has a maximum in the equilibrium and it does not correspond to the state where S_S peaks, the reservoir set must rise its entropy, similarly to case (I).

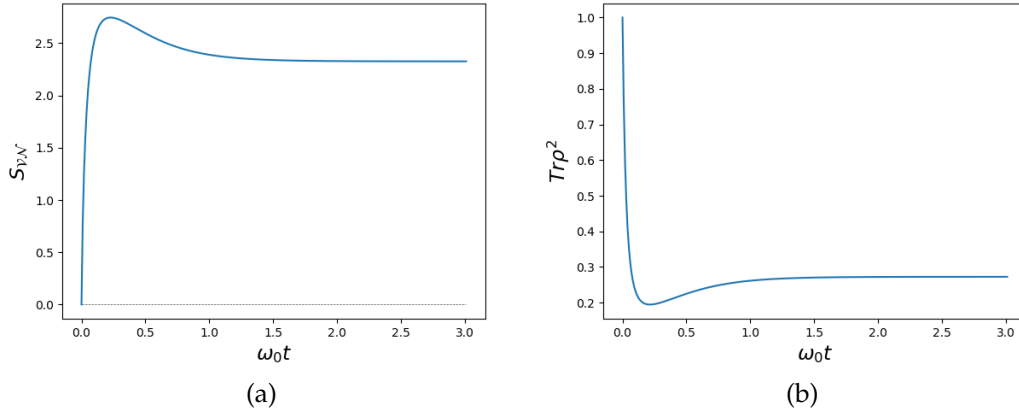


Figure 6: Evolution of S_{VN} (a) and $\text{Tr} \rho^2$ (b) for case (II): initial state $|\Psi(0)\rangle = 1/\sqrt{14}(3|2, e\rangle + |2, g\rangle + 2|1, e\rangle)$ with $\omega'_A = \omega'_c = 3\omega_0$, $\kappa_1 = \kappa_2 = d = 1.4\omega_0$, $\bar{n}_1 = 0.5$ and $\bar{n}_2 = 1$.

Figure 7 illustrates the decoherence process, where due to the interaction with the reservoirs, all coherence is leaked and the resulting state is no longer entangled, but a mixture of states. Nevertheless, as in this case $\bar{n}_i \neq 0$ and the stationary values of the populations are non-null, the JC interaction can still generate coherences between the $|n+1, g\rangle - |n, e\rangle$ states. Thus, among the initial coherences, the ρ_{2g1e} will be the only non-vanishing one.

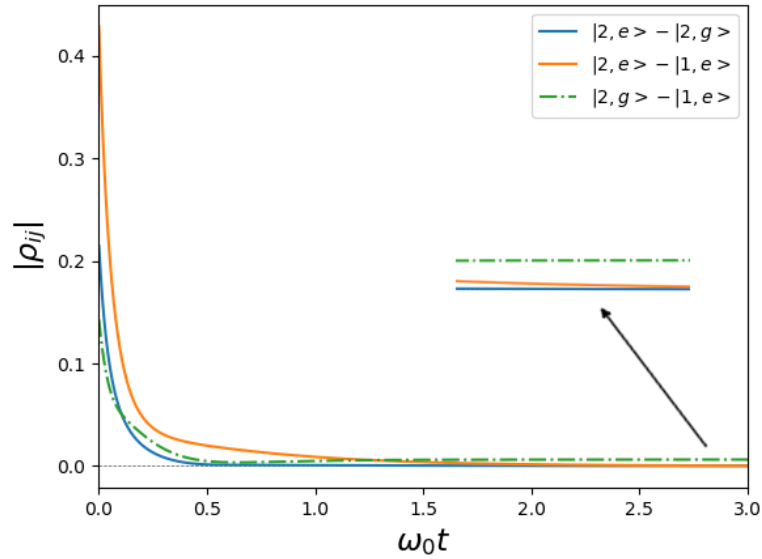


Figure 7: Evolution of initial coherences (modulus) for case (II): initial state $|\Psi(0)\rangle = 1/\sqrt{14}(3|2, e\rangle + |2, g\rangle + 2|1, e\rangle)$ with $\omega'_A = \omega'_c = 3\omega_0$, $\kappa_1 = \kappa_2 = d = 1.4\omega_0$, $\bar{n}_1 = 0.5$ and $\bar{n}_2 = 1$. Coherences ρ_{2e2g} and ρ_{2e1e} are plotted as solid lines, while ρ_{2g1e} is represented using dots and stripes.

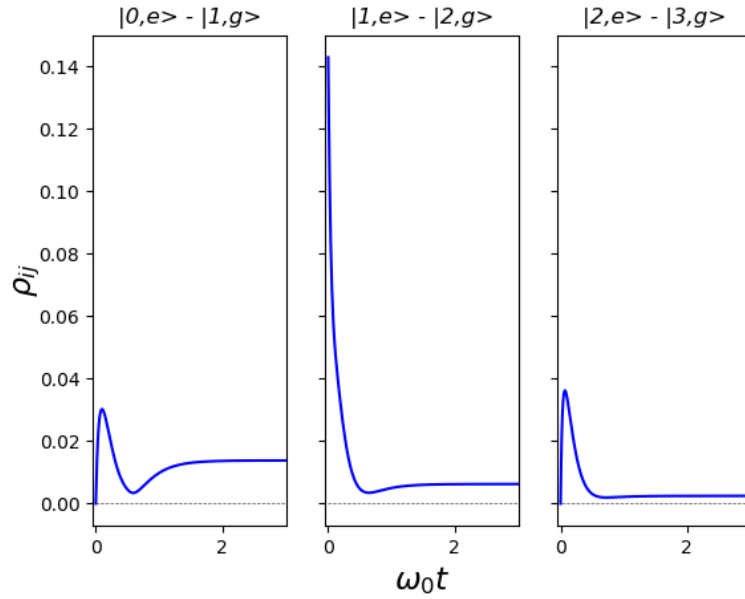


Figure 8: Evolution of the $\rho_{ne,n+1,g}$ coherences (imaginary part) for case (II): initial state $|\Psi(0)\rangle = 1/\sqrt{14}(3|2,e\rangle + |2,g\rangle + 2|1,e\rangle)$ with $\omega'_A = \omega'_c = 3\omega_0$, $\kappa_1 = \kappa_2 = d = 1.4\omega_0$, $\bar{n}_1 = 0.5$ and $\bar{n}_2 = 1$.

Regarding the $\rho_{ne,n+1,g}$ coherences, the matrix elements experience oscillations similar to case (I) due to the same causes; and will be purely imaginary as $d \in \Re$, although now they also reach a non-null stationary state as shown in Figure 8. We can see from (4.42) that this will happen when there is an equilibrium between the coherence received from the immediately higher-energy and lower-energy JC pairs of states $\{|n+1,e\rangle, |n+2,g\rangle\}$ and $\{|n-1,e\rangle, |ng\rangle\}$, respectively; the coherence transferred to those states (or lost due to the coupling with the reservoir, specially in the case of the one corresponding to the lowest energy pair $\{|0,e\rangle, |1,g\rangle\}$); and the one obtained from the imbalance on the $\{|ne\rangle, |n+1,g\rangle\}$ populations, which correspond to the second, third, first and fourth term of the mentioned equation, respectively.

5 Stochastic equation

Las ecuaciones estocásticas emergen como un posible medio para analizar el efecto que tiene la realización de una medida sobre un sistema en su estado; donde se considerará que la información se extrae de manera continua del sistema (una medida cuántica continua). Tras su derivación, aplicaremos estas ecuaciones para describir la evolución temporal del valor esperado del operador de posición, para el sistema S de la sección anterior y considerando dos situaciones diferentes: la medida simultánea sobre el átomo de dos niveles, estando ambas ligadas a la interacción con reservorios; y únicamente su medida teniendo en cuenta que el sistema de dos niveles experimenta decoherencia.

During a measurement, the used device subtracts information of the state of a specific system. Since the speed of light sets a limit to the velocity of any given particle, and therefore to the information transfer, it is clear that the process can not happen instantaneously. Moreover, while the measurement takes place, it is important to take into account that the system's state may be modified due to the interaction with the device. In order to describe such mechanisms, one has to consider a *continuous quantum measurement*, where the information is continually extracted from the system at a finite rate. This implies that the information collected goes to zero if the measurement time does. As a consequence of the randomness, which is intrinsic to the nature of the measurements, the system will be described by a stochastic equation. We will follow [3] for the derivation adding some clarifications, and will later describe the system shown in section 4 when the interaction between each reservoir and subsystem leads to a measurement of a Hermitian operator: the position for the harmonic oscillator and the operator $\zeta = \sigma_- + \sigma_+$ for the two-state atom. Furthermore, we will also consider the case of the measurement of the position when \mathcal{S}_2 undergoes a decoherence process.

5.1 Derivation

We will characterize a continuous measurement by dividing the time spent in intervals Δt , assuming a weak measurement is performed in each of them; and then take the limit $\Delta t \rightarrow dt$. The measured quantity X , which refers to an arbitrary observable (and hence Hermitian operator), will be considered to have a continuous spectrum $\{x\}$ and eigenstates $\{|x\rangle\}$, which are assumed to be orthogonal: $\langle x|x'\rangle = \delta(x - x')$. Then, each measurement will be estimated as a Gaussian-weighted sum of projectors onto the eigenstates of X , described by the operator

$$A(\alpha) = \left(\frac{4k\Delta t}{\pi}\right)^{1/4} \int_{-\infty}^{\infty} e^{-2k\Delta t(x-\alpha)^2} |x\rangle\langle x| dx. \quad (5.1)$$

Since α is a continuous index, there is a continuum of measurements results labelled by it. Expanding the initial state in the basis of X : $|\psi\rangle = \int \psi(x)|x\rangle dx$, the probability of getting α as a result of the measurement is given by

$$\mathcal{P}(\alpha) = \text{Tr}[A^\dagger(\alpha)A(\alpha)|\psi\rangle\langle\psi|] = \sqrt{\frac{4k\Delta t}{\pi}} \int_{-\infty}^{\infty} dx |\psi(x)|^2 e^{-4k\Delta t(x-\alpha)^2}. \quad (5.2)$$

We see that if Δt is small enough, the Gaussian is much broader than $\psi(x)$, and thereby $|\psi(x)|^2$ can be approximated by a delta function centered at the expectation value of the operator X :

$$\mathcal{P}(\alpha) \approx \sqrt{\frac{4k\Delta t}{\pi}} \int_{-\infty}^{\infty} dx \delta(x - \langle X \rangle) e^{-4k\Delta t(x-\alpha)^2} = \sqrt{\frac{4k\Delta t}{\pi}} e^{-4k\Delta t(\alpha - \langle X \rangle)^2}. \quad (5.3)$$

Nevertheless, the expectation value of the measurement is given by

$$\begin{aligned}\langle \alpha \rangle &= \int_{-\infty}^{\infty} d\alpha \alpha \mathcal{P}(\alpha) = \sqrt{\frac{4k\Delta t}{\pi}} \int_{-\infty}^{\infty} dx |\psi(x)|^2 \int_{-\infty}^{\infty} d\alpha \alpha e^{-4k\Delta t(x-\alpha)^2} \\ &= \int_{-\infty}^{\infty} dx x |\psi(x)|^2 = \langle X \rangle,\end{aligned}\quad (5.4)$$

and therefore, α can be effectively described by the stochastic variable

$$\alpha_s = \langle X \rangle + \frac{\Delta W}{(8k)^{1/2} \Delta t}, \quad (5.5)$$

where ΔW is a random, Gaussian variable with mean $\langle \Delta W \rangle = 0$ and variance Δt , described by the probability density

$$\mathcal{P}(\Delta W, \Delta t) = \frac{1}{(2\pi\Delta t)^{1/2}} e^{-(\Delta W)^2/2\Delta t}. \quad (5.6)$$

We will now consider the effect of a single measurement in the evolution of the system, taking into account that for all purposes $\alpha \simeq \alpha_s$:

$$|\psi(t + \Delta t)\rangle \propto A(\alpha) |\psi(t)\rangle \propto e^{-2k\Delta t(\alpha - X)^2} |\psi(t)\rangle \propto e^{-2k\Delta t X^2 + X[4k\langle X \rangle \Delta t + (2k)^{1/2} \Delta W]} |\psi(t)\rangle. \quad (5.7)$$

Expanding the exponential to first order in Δt and second order in W :

$$|\psi(t + \Delta t)\rangle \propto \{1 - 2k\Delta t X^2 + X[4k\langle X \rangle \Delta t + (2k)^{1/2} \Delta W + kX(\Delta W)^2]\} |\psi(t)\rangle. \quad (5.8)$$

Before taking the continuum limit $\Delta t \rightarrow dt$, we will examine the behaviour of $(\Delta W)^2$ in such situation. For doing so, let us introduce the central-limit theorem (CLT).

Theorem 1 *Let S_1, S_2, \dots, S_n be a set of random, independent and identically distributed variables of a distribution with mean μ and variance $\sigma^2 \neq 0$. Then, if n is sufficiently large, the random variable:*

$$\bar{S} = \frac{1}{n} \sum_{i=1}^n S_i$$

is approximately normally distributed with $\mu_{\bar{S}} = \mu$ and $\sigma_{\bar{S}} = \frac{\sigma^2}{n}$.

We shall now define the *Wiener process* $W(t)$, a random walk with arbitrarily small, independent steps taken arbitrarily often. If the random walk is symmetric, $W(t)$ will always give rise to a Gaussian distribution with $\langle W \rangle = 0$ in the continuum limit, where the number of steps goes to infinity as their size goes to zero and the conditions for the application of the CLT are satisfied. Therefore, if the variance is chosen to be t , the probability density for $W(t)$ will be analogous to (5.6), from where we can conclude:

$$\text{Var } W = \langle W^2 \rangle - \langle W \rangle^2 = t \quad \implies \langle W^2 \rangle = t. \quad (5.9)$$

Then, the *Wiener increment* is defined as

$$\Delta W(t) \equiv W(t + \Delta t) - W(t), \quad (5.10)$$

which will be a zero-mean, normally distributed variable with variance Δt . Therefore, similarly to equation (5.9), we would have $\langle\langle (\Delta W)^2 \rangle\rangle = \Delta t$, where the double brackets refer to an ensemble average over all possible ways the Wiener process can occur. Considering now the probability density function for $(\Delta W)^2$, which can be obtained from (5.6) by replacing $t \rightarrow \Delta t$ and $W \rightarrow \Delta W$ and performing the transformation

$$\int_{-\infty}^{\infty} \mathcal{P}(\Delta W) d(\Delta W) = 2 \int_0^{\infty} \mathcal{P}(\Delta W) d(\Delta W) = 2 \int_0^{\infty} \mathcal{P}[(\Delta W)^2] \frac{d(\Delta W)}{d[(\Delta W)^2]} d[(\Delta W)^2], \quad (5.11)$$

whose Jacobian is similar to $dx^{1/2}/dx = 1/2x^{1/2}$, allowing us to set

$$\mathcal{P}[(\Delta W)^2] = \frac{1}{[2\pi\Delta t(\Delta W)^2]^{1/2}} e^{-(\Delta W)^2/2\Delta t}, \quad (5.12)$$

which is a distribution with mean Δt and variance $2(\Delta t)^2$. We will consider now the sum of N Wiener increments of length $\Delta t_N = t/N$ between 0 and t . These are given by

$$\Delta W_n \equiv W[(n+1)\Delta t_N] - W(n\Delta t_N). \quad (5.13)$$

Now, the sum of the squared Wiener increments, which is a random walk of N steps of average t/N and variance $2t^2/N$; gives rise to a Gaussian random variable for large N with mean t and variance $2t^2/N$, according to the CLT. If we take the limit $N \rightarrow \infty$, the variance vanishes and the sum becomes t with certainty:

$$\int_0^t [dW(t')]^2 \equiv \lim_{N \rightarrow \infty} \sum_{n=0}^{N-1} (\Delta W_n)^2 = t = \int_0^t dt', \quad (5.14)$$

an equation that allows us to make the identification $dW^2 = dt$, the so called *Itô rule*. Therefore, dW is a random variable but dW^2 is not, as it has no variance when integrated over an arbitrary, finite interval. With this consideration, we can take the continuum limit in (5.8) to give

$$|\psi(t + dt)\rangle \propto \{1 - [kX^2 - 4kX\langle X \rangle]dt + (2k)^{1/2}X dW + \mathcal{O}(dt^2)\} |\psi(t)\rangle \equiv [1 + Y(X)] |\psi(t)\rangle. \quad (5.15)$$

However, the previous equation does not preserve the norm of $|\psi\rangle$. We can calculate one that does by normalizing $|\psi(t + dt)\rangle$ and expanding the result to first order in dt and second order in dW^2 :

$$|\psi'(t + dt)\rangle = \frac{|\psi(t + dt)\rangle}{\sqrt{\langle\psi(t + dt)|\psi(t + dt)\rangle}} = \frac{1 + Y}{\sqrt{\langle(1 + 2Y + Y^2)\rangle}} |\psi(t)\rangle. \quad (5.16)$$

We will first calculate the expectation value in the denominator:

$$\begin{aligned} \langle 1 + 2Y + Y^2 \rangle &= 1 + 2(-[k\langle X^2 \rangle - 4k\langle X \rangle^2]dt + (2k)^{1/2}\langle X \rangle dW) + 2k\langle X^2 \rangle dW^2 + \mathcal{O}(dt^2) \\ &= 1 + 8k\langle X \rangle^2 dt + 2(2k)^{1/2}\langle X \rangle dW + \mathcal{O}(dt^2). \end{aligned} \quad (5.17)$$

Thus, taking into account that $(1+z)^{-1/2} = 1 - \frac{1}{2}z + \frac{3}{8}z^2 + \dots$, we can substitute³ this result in the fraction in (5.16) for $z = \langle 2Y + Y^2 \rangle$ to give

$$(1+Y)\left(1 - \frac{z}{2} + \frac{3}{8}z^2\right) = 1 - 4k\langle X \rangle^2 dt - (2k)^{1/2}\langle X \rangle dW + 3k\langle X \rangle^2 dW^2 - [kX^2 - 4kX\langle X \rangle]dt + (2k)^{1/2}XdW - 2kX\langle X \rangle dW^2. \quad (5.18)$$

Hence, setting $|\psi(t+dt)\rangle = |\psi(t)\rangle + d|\psi\rangle$, the stochastic differential equation can be written as

$$d|\psi\rangle = \left\{ -k(X - \langle X \rangle)^2 dt + (2k)^{1/2}(X - \langle X \rangle)dW \right\} |\psi(t)\rangle, \quad (5.19)$$

which is known as the *stochastic Schrödinger equation* (SSE). It describes the evolution of a system in a time dt when the observer gets the measurement result

$$dy = \langle X \rangle dt + \frac{dW}{(8k)^{1/2}}. \quad (5.20)$$

Therefore, the measurement gives the expectation value $\langle X \rangle$ plus a random contribution due to the width of $\mathcal{P}(\alpha)$. The solution of the SSE for the evolution of the quantum state will show a progressive collapse of the state, in contrast with the instantaneous collapse that is assumed when a continuous measurement is not considered; and this evolution will be equivalent to the integration of $dy(t)$. Since it is possible to write the SSE in terms of $dy(t)$ by substituting $dW(dy, dt)$, the equation will give an evolution of the system conditioned by the measurement results. Therefore, the state $|\psi\rangle$ will evolve randomly and each stochastic solution $|\psi_i(t)\rangle$ is called *quantum trajectory*. We can find a SSE in terms of ρ by calculating $d\rho$ up to first order in dt . Abbreviating equation (5.19) as $d|\psi\rangle \equiv Q|\psi(t)\rangle$, $d\rho$ can be written as

$$\begin{aligned} d\rho &= \rho(t+dt) - \rho(t) = (|\psi(t) + d|\psi\rangle)(\langle\psi(t)| + d\langle\psi|) - |\psi(t)\rangle\langle\psi(t)| \\ &= d|\psi\rangle\langle\psi(t)| + |\psi(t)\rangle d\langle\psi| + d|\psi\rangle d\langle\psi| = Q\rho + \rho Q^\dagger + Q\rho Q^\dagger \\ &= 2k(X\rho X + \rho\langle X \rangle^2 - \langle X \rangle\{X, \rho\})dW^2 - k[\{X^2, \rho\} + 2\rho\langle X \rangle^2 - 2\langle X \rangle\{X, \rho\}]dt \\ &\quad + (2k)^{1/2}(\{X, \rho\} - 2\langle X \rangle\rho)dW \\ &= -k(\{X^2, \rho\} - 2X\rho X)dt + (2k)^{1/2}(\{X, \rho\} - 2\langle X \rangle\rho)dW, \end{aligned} \quad (5.21)$$

from where we obtain

$$d\rho = -k[X, [X, \rho]] + (2k)^{1/2}(X\rho + \rho X - 2\langle X \rangle\rho)dW. \quad (5.22)$$

Equations (5.19) and (5.22) account only for the effects of a measurement of the observable X in the system. To obtain the final form, we should add the partial derivative with respect to time, which for the state evolution gives

$$d|\psi\rangle = \left\{ -k(X - \langle X \rangle)^2 dt + (2k)^{1/2}(X - \langle X \rangle)dW + \frac{1}{i\hbar}Hdt \right\} |\psi(t)\rangle, \quad (5.23)$$

³The expansion will be implicitly assumed to be up to first order in dt from now on.

and in terms of the density operator we get

$$d\rho = -k[X, [X, \rho]] + (2k)^{1/2}(X\rho + \rho X - 2\langle X \rangle \rho)dW + \frac{1}{i\hbar}[H, \rho]dt. \quad (5.24)$$

The latter is a second order equation in ρ since $\langle X \rangle = \text{Tr } \rho X$, which is also known as the *stochastic master equation* (SME) and also defines a quantum trajectory $\rho_i(t)$. In order to calculate the average evolution $\bar{\rho}(t)$, it is important to remark that the previous equation is the continuum limit of the discrete relation of the form

$$\rho(t + \Delta t) = \rho(t) + \beta\Delta t + \gamma\Delta W(t). \quad (5.25)$$

Therefore, $\rho(t)$ depends on $\Delta W(t - \Delta t)$, but not on $W(t)$ and hence they are statistically independent, which implies $\langle\langle \rho dW \rangle\rangle = \langle\langle \rho \rangle\rangle \langle\langle dW \rangle\rangle = 0$. Then, the state averaged over all possible measurement results will follow the evolution given by

$$\frac{d\bar{\rho}}{dt} = -k[X, [X, \bar{\rho}]] + \frac{1}{i\hbar}[H, \bar{\rho}], \quad (5.26)$$

which would exactly coincide with the averaged sum of quantum trajectories $\bar{\rho}_{st}(t)$ when all possible trajectories are considered:

$$\bar{\rho}(t) = \lim_{N \rightarrow \infty} \bar{\rho}_{st}(t) = \lim_{N \rightarrow \infty} \frac{1}{N} \sum_{i=1}^N \rho_i(t). \quad (5.27)$$

Furthermore, equation (5.26) is exactly the master equation we would have obtained for a system whose interaction with a reservoir exclusively entails a measurement of an observable. As an example, the master equation for a harmonic oscillator will lead to the previous result if operators a and a^\dagger were substituted by the Hermitian position operator $X = \sqrt{\hbar/2m\omega_s}(a + a^\dagger)$ in the interacting term H_{SR} . Specifically, setting $\bar{n}_1 = \Delta_1 = 0$, it would be the result of applying this modification in the first line of (4.25). It is also possible to construct a similar density operator by considering the averaged sum of the projections over N quantum trajectories $|\psi_i(t)\rangle$:

$$\bar{\rho}_{|\psi\rangle_{st}}(t) = \frac{1}{N} \sum_{i=1}^N |\psi_i(t)\rangle \langle \psi_i(t)|, \quad (5.28)$$

where the subindex $|\psi\rangle_{st}$ indicates that it has been obtained considering stochastic evolutions of pure states; and which will strictly coincide with the ones obtained from (5.26) and (5.27) in the $N \rightarrow \infty$ limit.

5.2 Measurement on interacting systems via reservoir couplings

We will consider the setup described in section 4, but replacing $H_{S_1 R_1}$ and $H_{S_2 R_2}$ for sets of measurement interactions, specifically measurements of the position X and of

the Hermitian operator $\zeta = \sigma_+ + \sigma_-$, respectively:

$$\begin{aligned} H'_{S_1 R_1} &= \sum_j \hbar(b_j^* X r_j^\dagger + b_j X r_j) \equiv \hbar(X \Gamma_3^\dagger + X \Gamma_3), \\ H'_{S_2 R_2} &= \sum_{\mathbf{k}\lambda} \hbar(b_{\mathbf{k}\lambda}^* \zeta r_{\mathbf{k}\lambda}^\dagger + b_{\mathbf{k}\lambda} \zeta r_{\mathbf{k}\lambda}) \equiv \hbar(\zeta \Gamma_4^\dagger + \zeta \Gamma_4), \end{aligned} \quad (5.29)$$

where now b_j and $b_{\mathbf{k}\lambda}$ couple the j^{th} oscillator and \mathcal{S}_1 , and a photon with wave vector \mathbf{k} and polarization λ and \mathcal{S}_2 , in order to measure X and ζ , respectively.

5.2.1 SME derivation

Substituting the new $\mathcal{S}_i - \mathcal{R}_i$ interactions (5.29) in the Hamiltonian is formally equivalent to perform the replacement $(a, a^\dagger, \sigma_-, \sigma_+) \rightarrow (X, X, \zeta, \zeta)$ in (4.5). Hence, following the same steps for the derivation of the master equation and considering again the reservoirs' frequency spectrum to be a continuum, we can introduce

$$\begin{aligned} \kappa_3 &= \pi g(\omega_S) |b(\omega_S)|^2, & \kappa_4 &= \pi \sum_\lambda \int d^3 \mathbf{k} g(\mathbf{k}) |b(\mathbf{k}, \lambda)|^2 \delta(kc - \omega_S), \\ \Delta_3 &= P \int_0^\infty d\omega \frac{g(\omega) |b(\omega)|^2}{\omega_S - \omega}, & \Delta_4 &= \sum_\lambda P \int d^3 \mathbf{k} \frac{g(\mathbf{k}) |b(\mathbf{k}, \lambda)|^2}{\omega_S - kc}, \\ \Delta'_3 &= P \int_0^\infty d\omega \frac{g(\omega) |b(\omega)|^2}{\omega_S - \omega} \bar{n}_1(\omega, T), & \Delta'_4 &= \sum_\lambda P \int d^3 \mathbf{k} \frac{g(\mathbf{k}) |b(\mathbf{k}, \lambda)|^2}{\omega_S - kc} \bar{n}_2(kc, T), \end{aligned} \quad (5.30)$$

which allows us to write the master equation in the interaction picture (3.18) as

$$\begin{aligned} \dot{\tilde{\rho}} &= (\kappa_3 + i\Delta_3)(X\tilde{\rho}X - X^2\tilde{\rho}) + \text{h.c.} + (\kappa_4 + i\Delta_4)(\zeta\tilde{\rho}\zeta - \zeta^2\tilde{\rho}) + \text{h.c.} \\ &+ (\kappa_3\bar{n}_1 + i\Delta'_3)(2X\tilde{\rho}X - X^2\tilde{\rho} - \tilde{\rho}X^2) + \text{h.c.} + (\kappa_4\bar{n}_2 + i\Delta'_4)(2\zeta\tilde{\rho}\zeta - \zeta^2\tilde{\rho} - \tilde{\rho}\zeta^2) + \text{h.c.} \end{aligned} \quad (5.31)$$

Expanding the terms associated to \mathcal{S}_1 :

$$\begin{aligned} i) \quad &\kappa_3(2X\tilde{\rho}X - X^2\tilde{\rho} - \tilde{\rho}X^2) = -\kappa_3[X, [X, \tilde{\rho}]], \\ ii) \quad &i\Delta_3(X\tilde{\rho}X - X^2\tilde{\rho} - X\tilde{\rho}X + \tilde{\rho}X^2) = -i\Delta_3[X^2, \tilde{\rho}], \\ iii) \quad &\kappa_3\bar{n}_1(4X\tilde{\rho}X - 2X^2\tilde{\rho} - 2\tilde{\rho}X^2) = -2\kappa_3\bar{n}_1[X, [X, \tilde{\rho}]], \\ iv) \quad &i\Delta'_3(X\tilde{\rho}X - X^2\tilde{\rho} + X\tilde{\rho}X - \tilde{\rho}X^2 - X\tilde{\rho}X + \tilde{\rho}X^2 - X\tilde{\rho}X + X^2\tilde{\rho}) = 0. \end{aligned} \quad (5.32)$$

Since no commutation relations have been used, for \mathcal{S}_2 we obtain the same terms but replacing $(\kappa_3, \bar{n}_1, X) \rightarrow (\kappa_4, \bar{n}_2, \zeta)$. However, using the properties of the σ operators (4.21) we notice that

$$\zeta^2 = \sigma_-^2 + \sigma_+^2 + \{\sigma_-, \sigma_+\} = 1, \quad (5.33)$$

which along with (5.32) allows us to write the master equation in the interaction picture as

$$\dot{\tilde{\rho}} = -i\Delta_3[X^2, \tilde{\rho}] - \kappa_1(1 + 2\bar{n}_1)[X, [X, \tilde{\rho}]] + 2\kappa_4(1 + 2\bar{n}_2)(\zeta\tilde{\rho}\zeta - \tilde{\rho}). \quad (5.34)$$

Then, transforming the previous equation into the Schrödinger picture as in (4.24), we obtain the master equation:

$$\begin{aligned} \dot{\rho} = & -i\omega_s[a^\dagger a, \rho] - i\Delta_3[X^2, \rho] - \kappa_3(1+2\bar{n}_1)[X, [X, \rho]] \\ & - \frac{i}{2}\omega_s[\sigma_z, \rho] + 2\kappa_4(1+2\bar{n}_2)(\zeta\rho\zeta - \rho) + \{-id[a^\dagger\sigma_-, \rho] - id^*[a\sigma_+, \rho]\}. \end{aligned} \quad (5.35)$$

We see that in the absence of the stochastic terms ($dW_i = 0$), \bar{n}_1 and \bar{n}_2 would only increase the strength of the coupling κ_3 and κ_4 , respectively; and therefore their effects could be included in new coupling constants by setting $\gamma_1 = \kappa_3(1+2\bar{n}_1)$ and $\gamma_2 = \kappa_4(1+2\bar{n}_2)$. We will now include stochastic terms analogous to those in the general SME (5.24) and assume it is an adequate proposal for the measurement interaction we intend to describe. It is based on the fact that, with this procedure, the master equation we have obtained includes similar terms to those in the general SME averaged over the measurement record (5.26), plus a contribution dependent on Δ_3 . Therefore, Δ_3 might be a result of considering the detector to be some sort of reservoir, although a deeper analysis would be needed to evaluate the validity of these suppositions. Furthermore, considering the detector to be a reservoir is itself a questionable assertion, since reservoirs are assumed to remain unchanged by the interaction with the system; and it is this modification what allows a detector to measure. Therefore, what we intend to describe is a measuring device able to experience changes due to the interaction with a system, but being them small enough that they do not have any influence on the future evolution of \mathcal{S} , this is, that the Markoff approximation applies. The SME for this setup will be given by

$$\boxed{\begin{aligned} d\rho = & \{-i\omega_s[a^\dagger a, \rho] - i\Delta_3[X^2, \rho] - \gamma_1[X, [X, \rho]]\}dt + (2\gamma_1)^{1/2}(X\rho + \rho X - 2\langle X \rangle \rho)dW_1 \\ & \{-\frac{i}{2}\omega_s[\sigma_z, \rho] + 2\gamma_2(\zeta\rho\zeta - \rho)\}dt + (2\gamma_2)^{1/2}(\zeta\rho + \rho\zeta - 2\langle \zeta \rangle \rho)dW_2 \\ & + \{-id[a^\dagger\sigma_-, \rho] - id^*[a\sigma_+, \rho]\}dt. \end{aligned}} \quad (5.36)$$

If we write X in terms of a and a^\dagger as $X = \sqrt{\hbar/2m\omega_s}(a + a^\dagger) \equiv l_0(a + a^\dagger)$, where l_0 is a unit of length dependent on the mass m and the frequency ω_s of the harmonic oscillator, then the SME could be restated as

$$d\rho = \{-i\omega'_c[a^\dagger a, \rho] - l_0^2\{(\gamma_1 + i\Delta_3)(a^2 + (a^\dagger)^2)\rho + (\gamma_1 - i\Delta_3)\rho(a^2 + (a^\dagger)^2)\} + \dots\}dt + \dots, \quad (5.37)$$

where now $\omega'_c = \omega_s + 2l_0^2\Delta_3$. Hence, in this case the detuning term for \mathcal{S}_1 alters the frequency of this subsystem, but also effectively modifies the nature of the coupling constant for several terms; and as we see in (5.36) no detuning related to \mathcal{S}_2 appears. Projecting equation (5.36) onto the eigenstates of \mathcal{S} we find the evolution of an arbitrary matrix element, given by

$$\begin{aligned}
d\rho_{mfnh} = & - \left\{ [i\omega'_c(m-n) + 2\gamma_1 l_0^2(1+n+m)] \rho_{mfnh} \right. \\
& + \gamma_1 l_0^2 \left[\left(1 - i\frac{\Delta_3}{\gamma_1}\right) (\sqrt{n(n-1)}\rho_{m,n-2,h} + \sqrt{(n+1)(n+2)}\rho_{m,n+2,h}) \right. \\
& + \left. \left(1 + i\frac{\Delta_3}{\gamma_1}\right) (\sqrt{m(m-1)}\rho_{m-2,f,nh} + \sqrt{(m+1)(m+2)}\rho_{m+2,f,nh}) \right. \\
& - 2\left(\sqrt{n(m+1)}\rho_{m+1,f,n-1,h} + \sqrt{nm}\rho_{m-1,f,n-1,h} + \sqrt{(n+1)(m+1)}\rho_{m+1,f,n+1,h} \right. \\
& + \left. \left. \sqrt{(n+1)m}\rho_{m-1,f,n+1,h}\right) \right] \Big\} dt \\
& + (2\gamma_1)^{1/2} \left\{ \sqrt{n+1}\rho_{m,n+1,h} + \sqrt{n}\rho_{m,n-1,h} + \sqrt{m+1}\rho_{m+1,f,nh} + \sqrt{m}\rho_{m-1,f,nh} \right. \\
& - \left. 2\langle X \rangle \rho_{mfnh} \right\} dW_1 + \\
& - \left\{ \left[i\frac{\omega_S}{2}(\delta_{f1}\delta_{h0} - \delta_{f0}\delta_{h1}) + 2\gamma_2 \right] \rho_{mfnh} + \gamma_2 [\rho_{m,f-1,n,h-1} + \rho_{m,f-1,n,h+1} \right. \\
& + \left. \rho_{m,f+1,n,h+1} + \rho_{m,f+1,n,h-1}] \right\} dt \\
& + (2\gamma_2)^{1/2} \left\{ \rho_{m,f-1,nh} + \rho_{m,f+1,nh} + \rho_{mf,n,h-1} + \rho_{mf,n,h+1} - 2\langle \zeta \rangle \rho_{mfnh} \right\} dW_2 \\
& - id\sqrt{m}\rho_{m-1,f+1,nh} + id\sqrt{n+1}\rho_{mf,n+1,h-1} \\
& - id^*\sqrt{m+1}\rho_{m+1,f-1,nh} + id^*\sqrt{n}\rho_{mf,n-1,h+1}. \tag{5.38}
\end{aligned}$$

From the previous result, we can analyze the effects of the Δ_3 term in an arbitrary population:

$$\begin{aligned}
d\rho_{nfnf} = & \dots - i\Delta_3 l_0^2 [\sqrt{n(n-1)}\rho_{n-2,f,nf} + \sqrt{(n+1)(n+2)}\rho_{n+2,f,nf}] \\
& + i\Delta_3 l_0^2 [\sqrt{n(n-1)}\rho_{nf,n-2,f} + \sqrt{(n+1)(n+2)}\rho_{nf,n+2,f}] + \dots \\
= & \dots + 2i\Delta_3 l_0^2 \sqrt{n(n-1)}\rho_{nf,n-2,f} + 2i\Delta_3 l_0^2 \sqrt{(n+1)(n+2)}\rho_{nf,n+2,f} + \dots \tag{5.39}
\end{aligned}$$

We see that each of those terms are similar to the one we obtained in the first equation of (4.28), although now $\Delta_3 \in \mathfrak{R}$ by definition (5.30). In that case, the terms proportional to d were responsible for the transitions between the $|n, e\rangle$ and $|n+1, g\rangle$ states, which had the directionality needed to balance the unevenness in their populations. On the other hand, the Δ_3 terms will readjust the differences among the $|n, f\rangle$ and both $|n-2, f\rangle$ and $|n+2, f\rangle$ states. As it was explained while discussing (4.28), the mechanism first generates the coherences $\rho_{nf,n\pm 2,f}$ which will later affect the populations, and hence the population transfer will have some delay. This delay prevented the balance to be reached when we considered solely the JC interaction for a state $|\psi(t)\rangle = c_1(t)|n+1, e\rangle + c_2(t)|n, e\rangle$, which led to Rabi oscillations. The analogous result in this case would be an oscillation of a flow of populations from lower to higher n and vice versa, when $\Delta_3 \gg \gamma_1$; and will be more relevant the more unbalanced the populations of the initial state $|\psi(0)\rangle$ are. However, the Δ_3 term appears as a correction, and therefore is unlikely to be strong enough to drive the dynamics of a realistic physical system.

Analyzing the form of the Δ_3 term in (5.36), it can be seen that it could also be obtained if included in the Hamiltonian of the harmonic oscillator:

$$H'_{S_1} = \hbar\omega_s a^\dagger a + \hbar\Delta_3 X^2, \quad (5.40)$$

which corresponds to the Hamiltonian of a harmonic oscillator with a modified frequency ω'_s . This can be seen by writing the previous Hamiltonian in terms of X and P :

$$H'_{S_1} = \frac{\mathbf{P}^2}{2m} + \frac{1}{2}kX^2 + \hbar\Delta_3 X^2 \equiv \frac{\mathbf{P}^2}{2m} + \frac{1}{2}k'X^2 = \hbar\omega'_s a'^\dagger a', \quad (5.41)$$

where $k' = k + 2\hbar\Delta_3$ and therefore the new frequency is given by

$$\omega'_s = \sqrt{\frac{k'}{m}} = \sqrt{\omega_s^2 + \frac{2\hbar\Delta_3}{m}}. \quad (5.42)$$

Thus, we can write the previous ladder operators in terms of the new ones using the expressions for X and P , given by

$$X = \sqrt{\frac{\hbar}{2m\omega_s}}(a + a^\dagger) = \sqrt{\frac{\hbar}{2m\omega'_s}}(a' + a'^\dagger), \quad P = i\sqrt{\frac{\hbar m\omega_s}{2}}(a - a^\dagger) = i\sqrt{\frac{\hbar m\omega'_s}{2}}(a' - a'^\dagger), \quad (5.43)$$

from where we obtain

$$\begin{aligned} a &= \frac{1}{2} \left\{ a' \left[\left(\frac{\omega_s}{\omega'_s} \right)^{1/2} + \left(\frac{\omega'_s}{\omega_s} \right)^{1/2} \right] + a'^\dagger \left[\left(\frac{\omega_s}{\omega'_s} \right)^{1/2} - \left(\frac{\omega'_s}{\omega_s} \right)^{1/2} \right] \right\}, \\ a^\dagger &= \frac{1}{2} \left\{ a' \left[\left(\frac{\omega_s}{\omega'_s} \right)^{1/2} - \left(\frac{\omega'_s}{\omega_s} \right)^{1/2} \right] + a'^\dagger \left[\left(\frac{\omega_s}{\omega'_s} \right)^{1/2} + \left(\frac{\omega'_s}{\omega_s} \right)^{1/2} \right] \right\}. \end{aligned} \quad (5.44)$$

We could combine the Δ_3 term with H_{S_1} as in (5.41) and rewrite operators a and a^\dagger in the SME (5.36) in terms of a' and a'^\dagger using (5.44). In that case, we would project the SME onto the $|n', f\rangle$ states, the new eigenstates of the composite system, and continue the analysis from there. However, since it would lead to the appearance of a large number of terms depending on the new ladder operators, we will maintain the original formulation of the SME.

Finally, we would like to determine the SSE (5.23) for this system, in order to compare the averaged density matrices obtained using quantum trajectories $\rho_i(t)$ (5.27) and $|\psi_i(t)\rangle$ (5.28). However, for its derivation a different approach was followed, but analyzing the SME (5.36) and comparing it to the general expression (5.24), we find that the effects of the reservoir features appear through \bar{n}_i and Δ_3 , and hence we can take the following SSE as an assumption:

$$\begin{aligned} d|\psi\rangle &= \left\{ -\gamma_1(X - \langle X \rangle)^2 dt + (2\gamma_1)^{1/2}(X - \langle X \rangle)dW_1 - i\Delta_3 X^2 dt \right. \\ &\quad \left. - \gamma_2(\zeta - \langle \zeta \rangle)^2 dt + (2\gamma_2)^{1/2}(\zeta - \langle \zeta \rangle)dW_2 \right. \\ &\quad \left. - i[\omega_s(a^\dagger a + \frac{\sigma_z}{2}) + da^\dagger \sigma_- + d^* a \sigma_+] dt \right\} |\psi(t)\rangle, \end{aligned} \quad (5.45)$$

obtained by comparing the general SSE (5.23), the general SME (5.24) and the SME for this specific setup (5.36). If we calculate $d\rho$ in the same manner as in (5.21), keeping

terms up to first order in dt and neglecting terms proportional to the product $dW_1 dW_2$, we would obtain exactly the same SME (5.36). Therefore, it may be considered the right SSE linked to the SME we have derived. Nevertheless, since we know that when all trajectories are considered, both (5.27) and (5.28) must coincide, this equality will also serve as a test to determine the validity of the proposed equation.

5.2.2 Numerical solution

We will calculate the numerical solution of the SME (5.36) and evaluate the expectation value of X , which will serve as an indicator of the changes in the state of the system due to the measurement of X , but also of ζ since the H_{JC} interaction links \mathcal{S}_1 and \mathcal{S}_2 . As in previous sections, we will plot dimensionless quantities in order to focus only on the qualitative behaviour of the system.

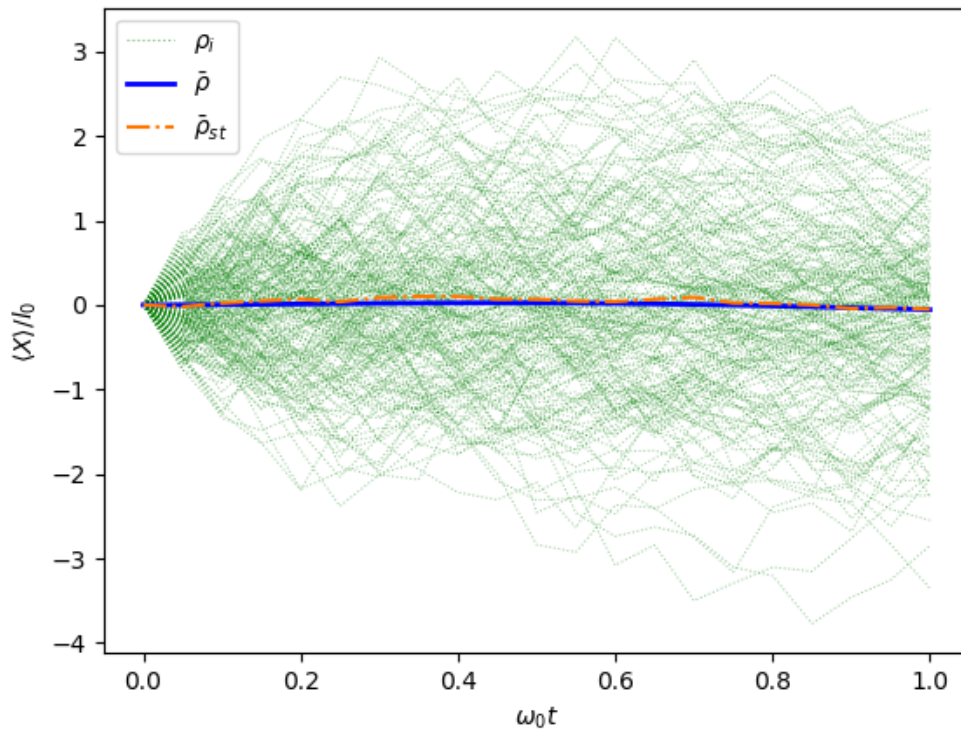


Figure 9: Evolution of $\langle X \rangle / l_0$ for $N = 200$ quantum trajectories ρ_i when ζ is simultaneously measured, using a step $\omega_0 \Delta t = 0.05$. The Gaussian distributions ΔW_i have zero mean and variance $\omega_0 \Delta t$. Each solution using a quantum trajectory ρ_i is plotted as a dashed line; their average $\bar{\rho}_{st}$ as dots and stripes; and the solution of the master equation with no stochastic terms (5.35), $\bar{\rho}$, as a solid line. The initial state is $|\psi(0)\rangle = |2, e\rangle$, and the parameters are $\omega_s = \omega_0$, $\gamma_1 = 0.1\omega_0/l_0^2$, $\gamma_2 = 0.5\omega_0$, $d = 0.1\omega_0$ and $\Delta_3 = 0.1\omega_0/l_0^2$.

In Figure 9 it can be seen that the evolution of $\langle X \rangle$ when using $\bar{\rho}_{st}$, the average of the quantum trajectories (5.27), approximately coincides with the one we obtain by employing the solution of the master equation with no stochastic terms $\bar{\rho}$ (5.35), when a suffi-

ciently large number of quantum trajectories ρ_i is considered.

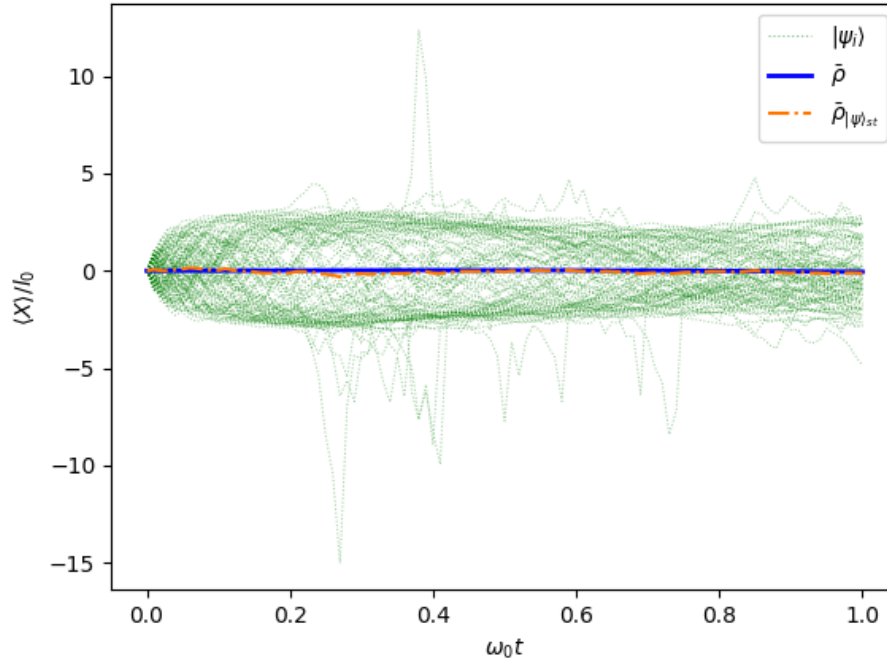


Figure 10: Evolution of $\langle X \rangle / l_0$ for $N = 100$ quantum trajectories $|\psi_i\rangle$ when ζ is simultaneously measured, using a step $\omega_0 \Delta t = 0.05$. The Gaussian distributions ΔW_i have zero mean and variance $\omega_0 \Delta t$. Each of the $N = 300$ solutions using a distinct $|\psi_i\rangle$ is plotted as a dashed line, the average over the projectors onto each trajectory $\bar{\rho}_{|\psi\rangle_{st}}$ as dots and stripes; and the solution of the master equation with no stochastic terms (5.35), $\bar{\rho}$, as a solid line. The initial state is $|\psi(0)\rangle = |2, e\rangle$, and the parameters are $\omega_s = \omega_0$, $\gamma_1 = 0.1\omega_0/l_0^2$, $\gamma_2 = 0.5\omega_0$, $d = 0.1\omega_0$ and $\Delta_3 = 0.1\omega_0/l_0^2$.

On the other hand, Figure 10 shows the correspondence between the stochastic density matrix $\bar{\rho}_{|\psi\rangle_{st}}$ (5.28), constructed from the projectors onto the quantum trajectories $|\psi_i\rangle$; and the non-stochastic master equation (5.35), since the evolution of $\langle X \rangle$ is relatively the same for both when enough trajectories are taken into account. Therefore, the equivalence among $\bar{\rho}_{st}$, $\bar{\rho}_{|\psi\rangle_{st}}$ and $\bar{\rho}$ when an adequate number of trajectories are considered has been verified. Hence, if possible, it would be recommendable to use a SSE to describe quantum trajectories, since the average result is equivalent and it is less demanding computationally. It can also be noticed that the variance in $\langle X \rangle$ is much larger when the evolution of single states is analyzed than when we use density operators. This might be explained by the fact that the ρ_i are already a collection of projectors onto several states; a weighted average in fact since generally there is a different probability of being in each state, and thereby some variance may be averaged out.

5.3 Measurement and interaction with a system under decoherence

We will consider the setup from section 4, but replacing the reservoir \mathcal{R}_1 by a position detector. Therefore, for \mathcal{S}_1 we will get the same terms that appear in (5.24), being now

X the position operator for the harmonic oscillator. We could derive the corresponding master equation and, since \mathcal{S}_2 is still interacting with \mathcal{R}_2 in the form of a decoherence process, as well as with \mathcal{S}_1 through the JC interaction, we would obtain the terms from the master equation (4.25) associated to these interactions, specifically the ones on the second and third line, respectively. Thereby, the stochastic master equation that describes this configuration is given by

$$\begin{aligned} \dot{\rho} = & -i\omega_S [a^\dagger a, \rho] - k [X, [X, \rho]] (2k)^{1/2} (X\rho + \rho X - 2\langle X \rangle \rho) dW_1 \\ & - \frac{i}{2} \omega'_A [\sigma_z, \rho] + \kappa_2 (2\sigma_- \rho \sigma_+ - \sigma_+ \sigma_- \rho - \rho \sigma_+ \sigma_-) + 2\kappa_2 \bar{n}_2 (\sigma_- \rho \sigma_+ + \sigma_+ \rho \sigma_- - \rho) \\ & - id [a^\dagger \sigma_-, \rho] - id^* [a \sigma_+, \rho], \end{aligned} \quad (5.46)$$

where again $\omega'_A = \omega_S + \Delta_2 + 2\Delta'_2$. In this case it is not possible to find a SSE, since the decoherence process leads to a mixture of states, making it indispensable to use ρ to describe the system.

5.3.1 Numerical solution

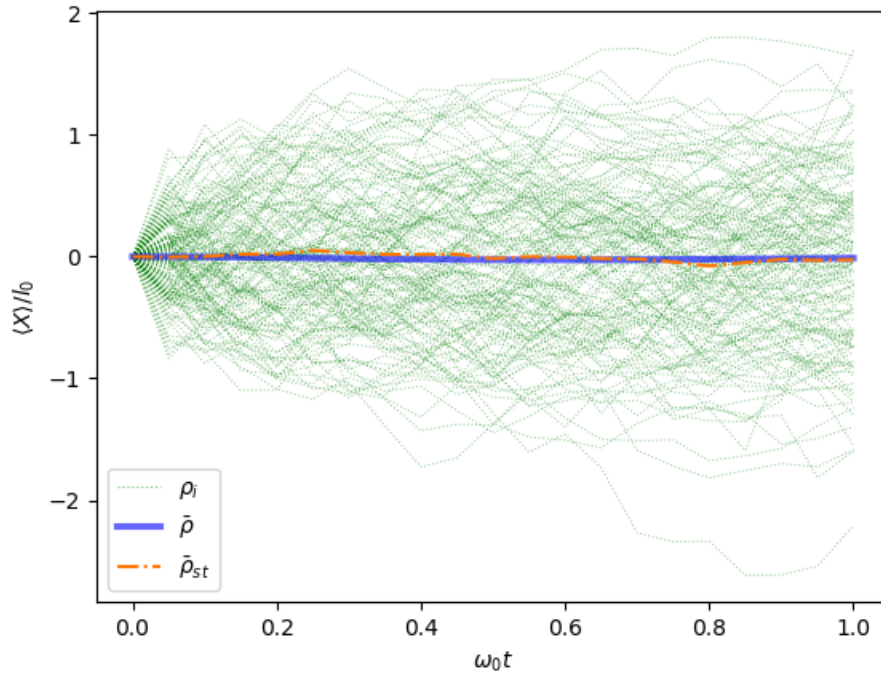


Figure 11: Evolution of $\langle X \rangle / l_0$ for $N = 150$ quantum trajectories ρ_i when \mathcal{S}_2 undergoes a decoherence process, using a step $\omega_0 \Delta t = 0.05$. The Gaussian distribution ΔW_1 has zero mean and variance $\omega_0 \Delta t$. Each solution using a quantum trajectory ρ_i is plotted as a dashed line; their average $\bar{\rho}_{st}$ as dots and stripes; and the solution of the master equation with no stochastic terms (5.35), $\bar{\rho}$, as a solid line. The initial state is $|\psi(0)\rangle = |2, e\rangle$, and the parameters are $\omega_S = \omega_0$, $k = 0.1\omega_0/l_0^2$, $\kappa_2 = 0.5\omega_0$, $d = 0.5\omega_0$ and $\bar{n}_2 = 1$.

As we see in Figure 11, the variance in the expectation value is lower than in the setup studied in section 5.2, due to the fact that there were two stochastic terms compared to the one existing in this case. Despite the fact that the stochastic term dW_2 does not directly influence the position, the JC term allows it to affect \mathcal{S}_1 through modifying \mathcal{S}_2 , and therefore alters the future evolution of the harmonic oscillator.

We notice that in both cases the average of $\langle X \rangle$ over the measurement record stays null. In order to justify this behaviour we should examine the equation for $\langle X \rangle$, given by

$$\begin{aligned} \langle X \rangle &= \text{Tr } \rho X = l_0 \sum_k p_k \langle \psi_k | (a + a^\dagger) | \psi_k \rangle = \sum_k p_k \left(\sum_{nf} \sqrt{n} c_{n-1,fk}^* c_{nfk} + \sum_{nf} \sqrt{n+1} c_{n+1,fk}^* c_{nfk} \right) \\ &= \sum_{nf} \sqrt{n+1} \sum_k p_k (c_{nfk}^* c_{n+1,fk} + c_{n+1,fk}^* c_{nfk}) = \sum_{nf} \sqrt{n+1} (\rho_{nf,n+1,f} + \rho_{n+1,f,nf}), \end{aligned} \quad (5.47)$$

where $c_{nfk} = \langle n, f | \psi_k \rangle$ and we have used the condition $n \geq 0$ in the fourth equality. Therefore, in order to increase $|\langle X \rangle|$ we would need coherences among the states $|nf\rangle$ and $|n \pm 1, f\rangle$. If we examine the SME for both cases, (5.36) and (5.46), we notice that the only terms able to generate the required coherences are $X\rho$ and ρX , which exclusively appear in the stochastic term proportional to dW_1 . This explains why $\langle X \rangle$ is generally non-null for each quantum trajectory, but turns out to be zero if we consider their average, since $\langle\langle dW_1 \rangle\rangle = 0$, or the respective non-stochastic master equation.

6 Conclusions

En relación a las ecuaciones maestras, a partir de los resultados obtenidos es posible realizar diversas conclusiones. En primer lugar, se comprueba en el caso (I), donde se estudió un estado inicial puro, no entrelazado a temperatura cero; el papel disipativo del proceso de decoherencia, que originaba un decaimiento al estado fundamental. Además, para el caso (II), donde consideramos un estado inicial puro y entrelazado; se corrobora la pérdida de coherencia debido a la interacción con el entorno, así como la aparición de estados estacionarios para las poblaciones y para las coherencias relacionadas con la interacción de Jaynes-Cummings, mostrando estos una variabilidad en función de las temperaturas de los reservorios. Finalmente, como consecuencia de la interacción de JC, observamos que el valor estacionario de las poblaciones de los estados $|n, e\rangle$ y $|n+1, g\rangle$ tienden a igualarse cuando la temperatura de los reservorios difiere.

Respecto a las ecuaciones estocásticas, observamos que en el caso de los dos subsistemas en interacción considerados, el efecto de dos medidas simultáneas está asociado a una mayor varianza en la evolución temporal del valor esperado del operador de posición, respecto a la obtenida en el caso de una única medida cuando el subsistema no medido experimenta un proceso de decoherencia. Por último, para el caso de las dos medidas, se comprueba que la media del registro de medidas de un observable es independiente de la utilización de una ecuación estocástica maestra o de Schrödinger, estando por tanto recomendado el uso de esta última cuando sea posible, debido a ser computacionalmente menos exigente.

Regarding the master equations, from the results obtained it is possible to draw several conclusions. First, the dissipative effects of the decoherence process has been observed in the decay to the ground state for case (I), where we considered an initial pure, non-entangled state at zero temperature. Furthermore, for case (II), characterized by an initial pure, entangled state at temperature different than zero; the coherence loss due to the coupling with the environment has been verified, as well as the appearance of stationary states for the populations and for the coherences related to the Jaynes-Cummings interaction, showing both a variability depending on the temperatures of the reservoirs. Moreover, as a consequence of the JC interaction, it has been perceived a tendency to even the populations of the $|n, e\rangle$ and $|n+1, g\rangle$ states when the temperatures of the reservoirs are distinct.

In relation to the stochastic equations, it has been observed that in the case of the two interacting subsystems considered, the effect of two simultaneous measurements is associated to a higher variance in the time evolution of the expectation value of the position operator, with respect to the one obtained in the case of a single measurement when the non-measured subsystem experiences a decoherence process. Finally, for the case of the two measurements, it has been confirmed that the average of the measurement record of an observable does not depend on the use of a SME or a SSE; being therefore recommended the use of the latter when possible, since it is less demanding computationally.

List of Figures

1	Evolution of populations for case (I)	16
2	Transition scheme for case (I)	17
3	Evolution of $S_{\mathcal{V}\mathcal{N}}$ and $\text{Tr } \rho^2$ for case (I)	17
4	Evolution of coherences (imaginary part) for case (I)	18
5	Evolution of populations for case (II)	19
6	Evolution of $S_{\mathcal{V}\mathcal{N}}$ and $\text{Tr } \rho^2$ for case (II)	21
7	Evolution of initial coherences (modulus) for case (II)	21
8	Evolution of the $\rho_{ne,n+1,g}$ coherences (imaginary part) for case (II)	22
9	Evolution of $\langle X \rangle / l_0$ using quantum trajectories ρ_i in the case of a simultaneous measurement of ζ	32
10	Evolution of $\langle X \rangle / l_0$ using quantum trajectories ψ_i in the case of a simultaneous measurement of ζ	33
11	Evolution of $\langle X \rangle / l_0$ using quantum trajectories ρ_i in the case of \mathcal{S}_2 undergoing a decoherence process	34

List of Tables

1	Possible transitions and transition rates	13
2	Corrections to the populations for different values of (\bar{n}_1, \bar{n}_2) for case (II)	20

References

- [1] Wojciech H.Zurek. Decoherence and the transition from quantum to classical – revisited. *Los Alamos Science*, (27):6–10, 2002.
- [2] Howard Carmichael. *An Open Systems Approach to Quantum Optics*. Springer-Verlag, Berlin Heidelberg, 1993.
- [3] Kurt Jacobs and Daniel A.Steck. A straightforward introduction to continuous quantum measurement. *Contemporary Physics*, 47(5):283–286, 10 2006.